


January 2012

Design of Contact Line Friction Measurement Machine Apparatus

Seyed Kamran Najafi

University of South Florida, skn@mail.usf.edu

Follow this and additional works at: <http://scholarcommons.usf.edu/etd>

 Part of the [Art Practice Commons](#), and the [Mechanical Engineering Commons](#)

Scholar Commons Citation

Najafi, Seyed Kamran, "Design of Contact Line Friction Measurement Machine Apparatus" (2012). *Graduate Theses and Dissertations*.
<http://scholarcommons.usf.edu/etd/4377>

This Thesis is brought to you for free and open access by the Graduate School at Scholar Commons. It has been accepted for inclusion in Graduate Theses and Dissertations by an authorized administrator of Scholar Commons. For more information, please contact scholarcommons@usf.edu.

Design of Contact Line Friction
Measurement Machine Apparatus

by

Seyed Kamran Najafi

A thesis submitted in partial fulfillment
of the requirements for the degree of
Master of Science in Mechanical Engineering
Department of Mechanical Engineering
College of Engineering
University of South Florida

Major Professor: Nathan Crane, Ph.D.
Muhammad Rahman, Ph.D.
Rasim Guldiken, Ph.D.

Date of Approval:
November 5, 2012

Keywords: Actuation force, Pinning force, Electrowetting,
Modeling, Enclosure

Copyright © 2012, Seyed Kamran Najafi

DEDICATION

This is the story of a young engineer that has always loved to invent new toys with all the junk that he found since he was 6 years old and his passion for being an engineer was formed while he was watching his father work for an engineering company. It was cool to see his father speak in other languages and make connections with other people around the world, as well as getting to know new and different cultures. When my father was taking me with him to visit different projects of his where he was involved in making power plants, I felt that this was amazing how they can make huge turbines and assemble them all together to generate electricity, and by this they help humanity. This became a dream for me to become an engineer; however, it wasn't easy! I always believed in my intelligence and this reason prevented me from working hard on my goals, because I could figure out problems quickly but not very deeply. My undergraduate in manufacturing engineering was pretty interesting and I learned a lot that is very helpful for my career. I could say it was not a big success, but I had a lot of fun and learned a lot about life which now I find them very helpful. After that an immigration opportunity came up for me to travel to a new country. I was thinking about my future and I had to sacrifice a lot of things I cared about in order to have a better life. Immigration is not easy at all but with the support

of my family we were able to find our way. I had a hard time in settling down and in getting to graduate school but once I started my master's program my life got better and better and now I am so happy. My parents are the best; I can't imagine any sacrifices that they didn't make to help me and my sister to be successful. I owe them for any happiness or success that I achieve in my life and I am very grateful for them taking care of me and not leaving me alone, even in the hardest time of my life, thus I dedicate this thesis to my mother, father and sister. I also thank my good friends in Iran: Azadeh, Farzin, Shahram, Ashkan, Flora and my dear grandmother that were giving me hope and making me happy even from long distance. I appreciate Nick, Ben, Barbara, Ryan, Mehdi and everyone who helped me with the writing of this thesis.

ACKNOWLEDGMENTS

I appreciate Dr. Nathan Crane for his support and for teaching me valuable lessons and sharing his experiences with me on this project. I am happy for this opportunity to work in a very educated group and meet absolutely intelligent people on a very exciting project. Special thanks go to my committee members, Dr. Rahman and Dr. Guldiken to helping me during my master's program. I am also grateful of the other project members, Timo and Qi for helping me during this design project. Finally it was a pleasure to meet Jose, Sean and Sam in our lab.

TABLE OF CONTENTS

LIST OF TABLES	iii
LIST OF FIGURES	iv
ABSTRACT	vi
CHAPTER 1: INTRODUCTION	1
1.1 Contacting Angle Definition	1
1.2 What is Electrowetting	4
1.3 Measuring of Contact Angle Hysteresis	4
1.3.1 Captive Needle	5
1.3.2 Tilted Plate	6
1.4 Direct Pinning Force Measurement	7
CHAPTER 2: DESIGN OF THE MEASUREMENT MACHINE	9
2.1 Functionality	9
2.1.1 Actuation Force	10
2.1.2 Force Measurement	10
2.1.3 Motion Control	11
2.1.4 Adjustability	11
2.1.5 Monitoring	12
2.2 Design Concepts	13
2.3 Linear Motion	16
2.4 Controller	16
2.5 Measurement Force Sensor	17
2.6 Vibration Isolation	19
2.6.1 Air Table	19
2.6.2 Breadboard	20
2.7 Hydrophobic Substrate	21
2.8 Vacuum Lifter System	22
2.9 Structure	24
2.10 Observation	25
2.11 Conclusion	26
CHAPTER 3: DESIGN OF CLEAN BOX	28
3.1 Concept	28
3.2 Transparent Box	29

3.3 Enclosure Structure	30
3.4 Clean Room	33
3.4.1 Positive Air Flow	34
CHAPTER 4: PROCESS.....	37
4.1 Process of Measurement.....	37
4.1.1 Preparation	37
4.1.2 Programming	39
4.2 Formula and Calculations	41
4.3 Test Configurations	42
4.3.1 The Interfacial Tensions Between Liquid and Vapor	42
4.3.2 Droplet	43
4.3.3 Motion	43
4.4 Programming	44
CHAPTER 5: RESULTS	45
5.1 Theoretical Measurement vs. Direct Measurement.....	45
5.2 Comparison.....	48
5.2.1 Force Measurement Mechanism.....	49
5.2.2 Noise and Smooth Motion	49
5.2.3 Accessibility.....	50
5.2.4 Transparent Box.....	51
5.2.5 Clean Room	51
5.2.6 Flexibility	51
5.2.7 Price and Transportation.....	52
CHAPTER 6: CONCLUSION	53
6.1 Conclusion	53
6.2 Future Work.....	53
REFERENCES	55
APPENDICES.....	58
Appendix A Components Specifications.....	59
Appendix B Customized Components Drawing	64
Appendix C Copyright and Permissions	67

LIST OF TABLES

Table 1: Component List of Measurement Machine.	26
Table 2: The Box Components List.....	32
Table 3: Controlling Commands	39
Table 4: Measuring the Advancing and Receding Contact Angle with Captive Needle Method.....	46
Table 5: Measuring the Advancing and Receding Contact Angle with Tilting Method.....	46
Table 6: Measuring the Contact Friction Force with Direct Method	47
Table A: Stage Specifications	59
Table B: Camera Specifications	60
Table C: Rail Structure Specifications	61
Table D: Rail Carriers Specifications	61
Table E: MEMS Sensor Specifications.....	62
Table F: Breadboard Specifications.....	62
Table G: Manual Positioner Specifications	63

LIST OF FIGURES

Figure 1: A Droplet on the Hydrophilic Surface.....	2
Figure 2: A Droplet on the Hydrophobic Surface	2
Figure 3: Advancing Process with Captive Needle Method.....	5
Figure 4: Receding Process with Captive Needle Method	6
Figure 5: Contacting Angle by Tilting Method.....	7
Figure 6: Function of Components	12
Figure 7: Stage Moves the Substrate under the Droplet and Causes Dragging Force	13
Figure 8: Fiber Wire is Attached to the Top Glass Plate and Sensor	14
Figure 9: Carriers and X, Y Manual Positioner	14
Figure 10: Design Concept.....	15
Figure 11: MEMS Sensor (Right) - Tip of Sensor (Left)	18
Figure 12: Isolation Support System.....	20
Figure 13: Sandwich Breadboard.....	21
Figure 14: Picking up the Top Glass Plate with Fiber Chuck in a 3d Model.....	23
Figure 15: Vacuum Lifter	24
Figure 16: Design Prototype	27
Figure 17: Assembled Machine.....	27
Figure 18: Front Box View Prototype (Left) - Right Box View Prototype (Right) .	30

Figure 19: Structure Prototype.....	32
Figure 20: Assembled Box	33
Figure 21: Fan (Left) Filter in The Customized Box (Right).....	35
Figure 22: Isometric View of the Complete Machine Prototype.....	36
Figure 23: Programming the Stage.....	40
Figure 24: Programming Stage with Jogging Window	40
Figure 25: Velocity-Time Diagram	42
Figure 26: Speed Stability at 10 $\mu\text{m/s}$ – Sampling 50 Hz.....	44
Figure 27: Force (N) vs. Distance (mm) on Volume 41 μl by Customized Machine	48
Figure A: Focal Lens Length.....	60
Figure B: Sensor Mount Block	64
Figure C: Camera Mounting Bracket to Micro Positioner	64
Figure D: Under Stage Bracket.....	65
Figure E: Vacuum Lifter Mount.....	65
Figure F: Micro Positioner Mounting Bracket to Carrier	66
Figure G: Top Stage Bracket	66
Figure H: Permission for Figure 12 Courtesy of Newport Co	67
Figure I: Permission for Figure 11 Courtesy of Nanoscience Instruments Co	68
Figure J: Permission for Figure A Courtesy of Edmund Optics Co.....	69
Figure K: Direct Email for Figure 26 Courtesy of Newport Co	70

ABSTRACT

The purpose of this project is to design and manufacture a high precision machine to directly measure the surface force of fluids. Knowing how to move droplets easier with less resistance can increase the potential of a wide range of applications and improve the performance of things such as self-assembly applications. This machine has the ability to measure forces of up to $\pm 100 \mu\text{N}$ with a MEMS based sensor. The motion system on this machine moves a substrate underneath of a droplet for 100 mm and applies dragging force to the sensor. It moves with a controlled speed with high accuracy and repeatability. The machine also consists of three manual, three axis controls for positioning key components for observation, control of the air vacuum lifter, and adjustment of the sensor position. There is also an enclosure box that provides visibility to operate and protects the inside environment from dirt during process and also by applying positive air flow during setting up with open windows. The test components were designed to provide maximum flexibility to adjust the setup. A camera in the machine contributes to collect data during the test progress and has the ability to capture pictures and record videos.

CHAPTER 1: INTRODUCTION

This chapter contains basic information about surface tension force and traditional methods that are used to measure it. The potential use of this measurement will be covered and how we improved the measurement to new direct method and what are the advantages of this new method.

1.1 Contacting Angle Definition

Wetting a droplet on different surfaces has different effects. For instance when the droplet rests on a horizontal glass plate without any coating, it spreads widely on the surface. Yet the same droplet does not spread similarly on a brass surface and looks more spherical [1]. A ratio of a droplet and the properties of the surface material are effective in the shaping of the droplet. According to Thomas Young's theory, these phenomena result from interfacial tension between gas and solid, liquid and solid, and liquid and gas. These interfacial tensions affect the contacting angle between the droplet and the surface.[2], [3] If a water droplet wets the surface, the surface is called hydrophilic, from Latin, meaning "water loving". The contact angle of static water with this surface will be less than zero degrees. If the surface repels it, the contacting angle would be more than 90° and this surface is called hydrophobic, which is Latin for "water

fearing.” This contact angle measurement depends on the properties of the materials. Molecules of hydrophilic materials are polarized and tend to be dissolved in water; conversely, this fact is reversed for hydrophobic molecules. They are not polarized, so water can “slip” on a hydrophobic surface. [4]



Figure 1: A Droplet on the Hydrophilic Surface

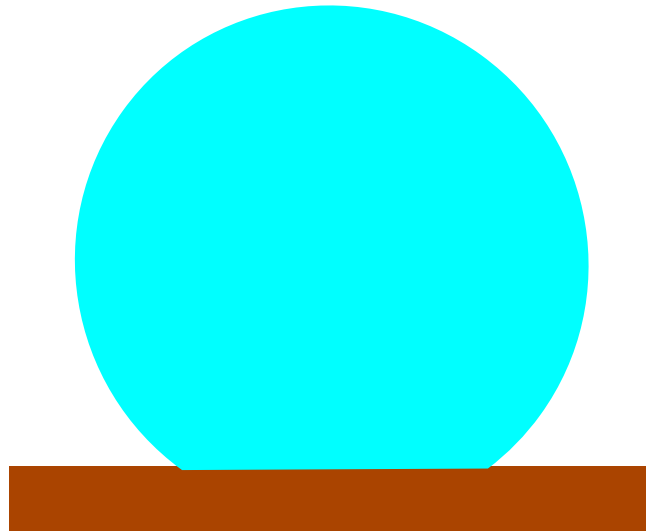


Figure 2: A Droplet on the Hydrophobic Surface

Before water slips over a hydrophobic substrate, there is a resistant force that needs to be overcome in order to start motion of the contact line. Thus the resisting force can be defined as the hysteresis force. By measuring the advancing and receding contact angle between droplet and surface, and applying the Furmidge's equation the hysteresis force can be calculated. [5]

$$(\rho V \sin(\theta_e) = W_{drop} \gamma_{LV} (\cos \theta_{rec} - \cos \theta_{adv})) \quad (1)$$

Young's surface free energy formula is given by

$$\gamma_{SL} - \gamma_{SV} + \gamma_{LV} \cos \theta_0 = \delta_E \quad (2)$$

where γ_{SL} is the interfacial tension between solid and liquid, γ_{SV} is the tension between solid and vapor and γ_{LV} is the tension between liquid and vapor. Referring to Young's equation $\delta_E = 0$ and $\gamma_{LV} \cos \theta_0 = W$, which is the work done by the adhesion of the fluid to the substrate. The pinning force can be defined by following this equation by the method of tilting angle, noting that θ_e is the normal angle on the surface, mg is the weight of droplet, L is the contacting length between droplet and surface, γ_{LV} are the interfacial tensions between liquid and vapor and θ_{rec} and θ_{adv} are the receding and advancing angles. [6]

$$F_{Hys} = \gamma_{LV} (\cos \theta_{rec} - \cos \theta_{adv}) \quad (3)$$

1.2 What is Electrowetting

Electrowetting is a phenomenon that describes the change in wetting on a droplet due to an applied electric field. Applying potential difference to a droplet and electrowetting substrate causes the contact angles to change. The electrowetting substrate can be physically designed or positioned in a way that the angles at the two ends of droplet are different. By rendering a net force to the droplet in the direction where the droplet assumes smaller contact angle. Electrowetting can be used on a variety of technologies such as microfluidic devices for bio applications as well as on displays for different devices such as smart phones and tablets with higher resolution and less power consumption than conventional technologies. [1], [4], [7]

Electrowetting has a lot of usage in the medical field as well. Due to a change of tension force on optical lenses, the focal distance is adjustable. Large use of this technology in requires more research in this field to develop the knowledge of this method in order to achieve more accurate results. One of the most important matters in electrowetting is to find the resisting friction to motion of the droplet.

1.3 Measuring of Contact Angle Hysteresis

In respect to formula 3, in order to find the hysteresis force that needs to move the droplet, the advancing and receding angles need to be measured. Here we

talk about two different dynamic methods to measure these contacting angles. For these dynamic methods either the shape of droplet would change, and during the process the two contacting ends between the surface and the liquid will be measured. It should be noted that with this method the contact angle will be measured during a process of changing the volume of the droplet or its shape. [8]

1.3.1 Captive Needle

In this method a programmable pump can be used to deposit and withdraw a certain amount of fluid to form a droplet. The needle size with this method should be very small in comparison with the diameter of the droplet. It is also important to perform the process of adding and removing the water slowly to minimize viscous effects. For this method, the droplet is added to a horizontal hydrophobic substrate via a small needle. Water is then added to the substrate at a constant rate. While the volume of the droplet changes, pictures are recorded of its formation. There are some software such as IMAGEJ that are able to measure contacting angle hysteresis. [8]

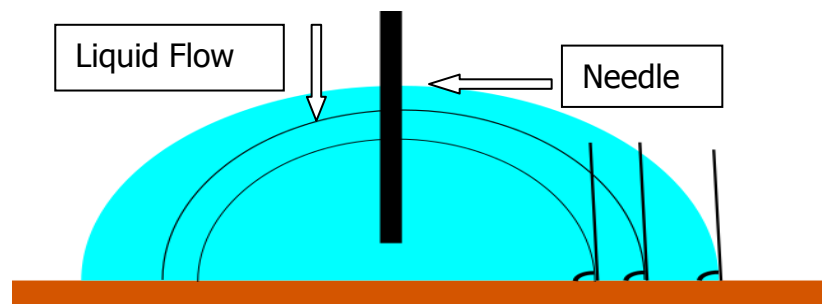


Figure 3: Advancing Process with Captive Needle Method

By pumping water droplet on a substrate with constant deposit rate, advancing contact angle can be defined at certain volume before end boundaries of droplet move. For measuring the receding contact angle, reverse process as advancing contact angle the water droplet will be drained and decrease the volume of droplet. In conclusion, the adding process gives the advancing angle and draining supplies the receding angle.[9] The difference between advancing and receding angles gives the surface roughness. Unlike the advancing angle, it is known that the receding angle is not appropriate to find surface energy. [8]

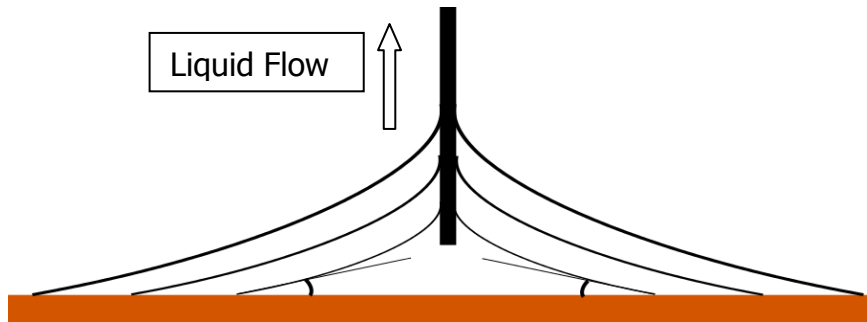


Figure 4: Receding Process with Captive Needle Method

1.3.2 Tilted Plate

This is the traditional method in which the substrate is tilted in relation to the normal of the Earth's gravitational field. The contacting angle hysteresis is measured at the angle right before the droplet starts moving. Droplets with bigger volume slide more easily with smaller tilt. The advancing angle is the rear of the droplet and the receding angle would be the front toward the tilted direction. The problem with this method is that when the substrate tilts the left

side of the droplet might start moving while the right side is still attached to the surface. That means the side that causes the droplet to move has less surface tension. By changing the volume, contacting angles will change but according to equation (3) this will not affect the hysteresis force. Increasing the droplet volume causes the surface to separate from the advancing angle and decreasing the volume has the reverse results. [10]

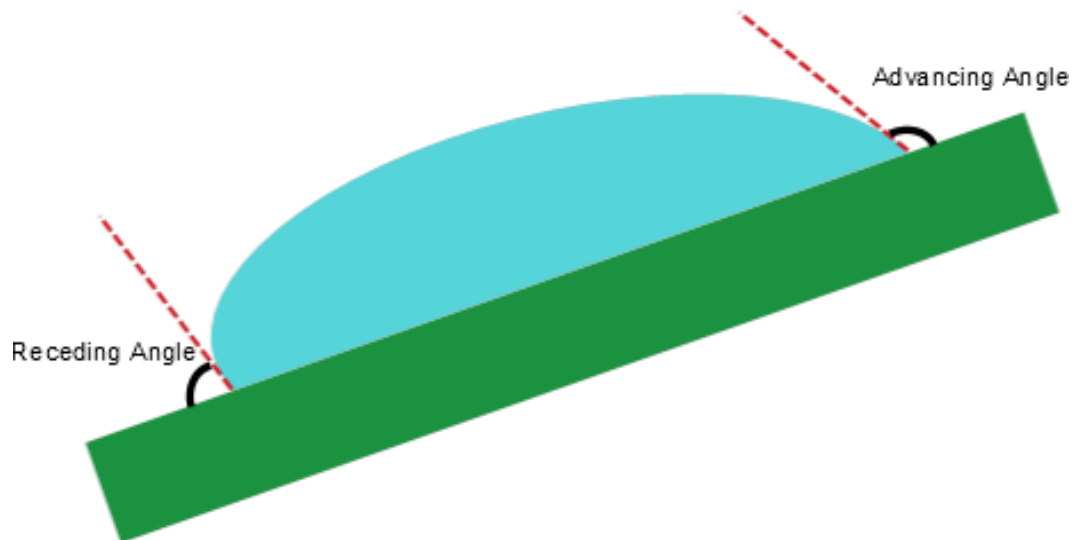


Figure 5: Contacting Angle by Tilting Method

1.4 Direct Pinning Force Measurement

Thanks to technological improvements, nowadays we can use sensors with high precision to measure small forces, which is exactly what we need in our research into the field of electrowetting. Measuring the pinning force between liquid and solid surfaces is more accurate with direct force sensing. That means no contacting angle needs to be measured to be used in the related equations and less errors would be involved during measurement. This thesis covers the design

of an X-axis (which induces motion to a substrate) and an adjustable setup for the sensor. Another design task was in setting up the tests. According to initial research data it was noted that a new generation of MEMS sensors are in the market that are perfect for our research. The challenge in this project is to minimize all the adverse effects due to the environment in order to capture the most accurate data. This requires all the components to fit together precisely, with a non-complicated design. It is also important to prevent direct handling of the set up due to the high sensitivity of the sensors, which may be damaged easily. This thesis also covers the process of fabrication as well as the test results.

CHAPTER 2: DESIGN OF THE MEASUREMENT MACHINE

In this chapter you will discover required functions that are required for designing of this machine and you will discover how the concept was figured. Furthermore different components that are used in this machine will be reviewed and how they are being used in the machine and what are their specifications. Also we discuss more about how other ideas didn't work and what the challenges were during designing process.

2.1 Functionality

The idea of designing this machine came through a need of a direct measurement of contact life friction or actuation electrowetting force of a water droplet over a hydrophobic substrate. For this purpose a list of functions are required to accomplish the concept of design. These functions are:

1. Providing actuation force
2. Measuring the actuation force
3. Controlling and changing the actuation force
4. Set up and adjustability
5. Monitoring the test and observing the setup

2.1.1 Actuation Force

The machine should be able to supply either electrowetting actuation force or contact line friction. A motion system can provide variety of the contact line friction by applying different inputs. The velocity range on the motion system should be between 10 $\mu\text{m/s}$ and up to a certain point where the contact line friction is not excessive on a linear direction for 100 mm. Also minimum acceleration recommendation is around 40 $\mu\text{m/s}^2$ and maximum acceleration should follow same principles as maximum velocity. Furthermore accuracy of this motion is important criteria and it suggests to be around 6 μm and repeatability could be important when there are continues test rounds with same displacement range and it offers to be 4 μm in bi-direction. Due to this high precision process, repeatability and accuracy are a big concern in the motion system. Additionally, a strip substrate with patterns of oxide aluminum and a layer of Cytop coating can be attached to conductors on each side of the substrate. By applying differential voltage, actuation can be provided to move the water droplet. [11]

2.1.2 Force Measurement

The machine also needs a precision force measurement system that is able to record the actuation force directly. Following that concept a method is required to transfer the applying force from the droplet to a sensor that is able measure the tensile force in proper scale. The idea is to use a sensor that is able to

measure the actuation force up to 2000 μN and 50 $\mu\text{N/V}$ sensitivity. In order to increase the accuracy of force measurement, negative factors need to be reduced. For instance, vibration isolation is helpful to control any vibration from the environment. Moreover, providing an enclosure box during the test would be helpful against air pollution and sound vibration. Applying a positive air flow up to certain pressure that does not have bad influence on the setup helps to keep the enclosure room isolated from air pollution while the box is open and the operator is working with the implements.

2.1.3 Motion Control

Another factor for this machine is that it needs to have control over the applying force by changing the motion parameters in respect to the measurement system capability. Also, it is helpful that the controller should provide feedback of velocity, position, and acceleration of the motion.

2.1.4 Adjustability

Coordinating the components and aligning them is a big concern for components that may need to be set up after or before each test. The advantage of using adjustable components such as a micropositioner are that they are accurate when compared with hand involved operation can cause less accidental mistakes and prefer to travel in 1" travel range on X, Y, Z axis for the sensor and lifting components and X, Z axes for camera.

2.1.5 Monitoring

Having an observation system helps to monitor and study the droplet behavior during the process. Also, this observation system helps with sensitive set up that require more precision. For vertical field of view of 2.5 cm x 2.5 cm to the substrate, a lens with compatible focal length is required to provide high level of image quality with decent tolerance and simple installation.[12]

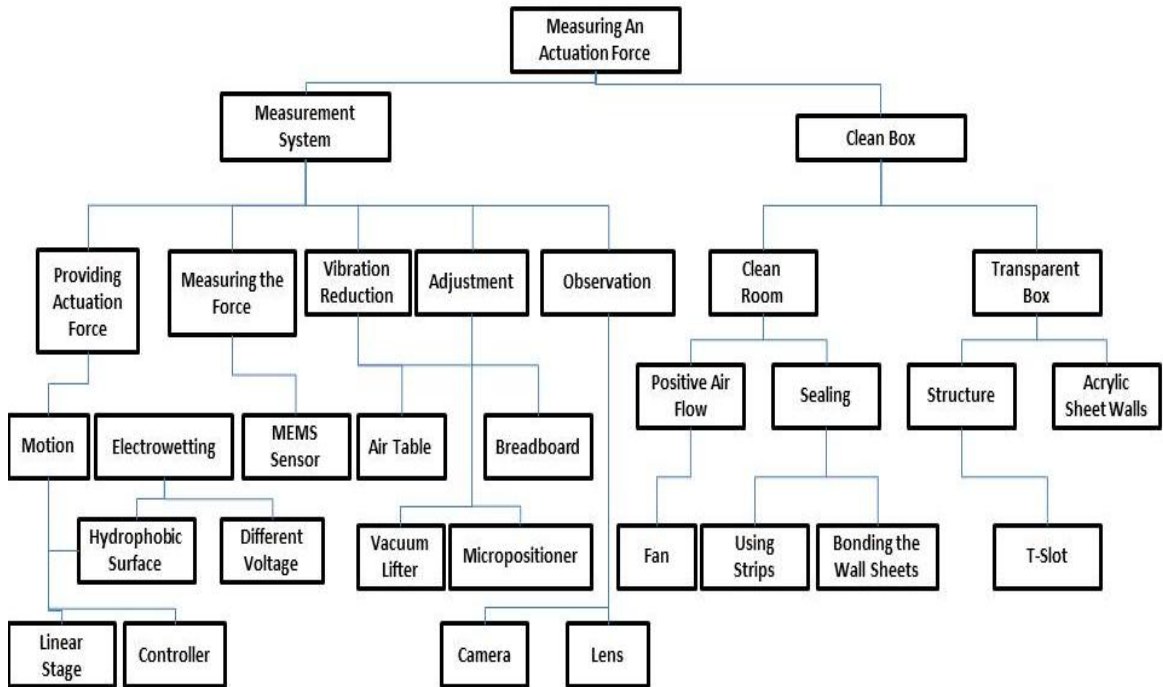


Figure 6: Function of Components

2.2 Design Concepts

The main purpose of designing this machine is to measure the pinning force and actuation force between the droplet and the solid surface directly. The basic concept is to apply a dragging force by a motion system to the droplet and thus measure the contact line friction. However, this actuation can come from an electrowetting process by applying a differential voltage to a resistive hydrophobic substrate with aluminum oxide layers pattern along it.[11] A MEMS sensor is able to measure tensile forces in micro scale. So the challenge is to connect the droplet to the sensor on horizontal alignment. A typical square glass plate rests on top of the droplet. The glass plate bonds to an end of a fiber wire and the other end of the wire bonds to the tip of the sensor and can be horizontally leveled by using a micro positioner. Due to higher surface tension between the droplet and the glass plate, than between the droplet and the substrate, these two objects will stay connected together while the droplet slides on the substrate. This connection between the glass plate and the droplet causes a drag force, thus the wire pulls the tip of the MEMS based sensor (Figure 7).

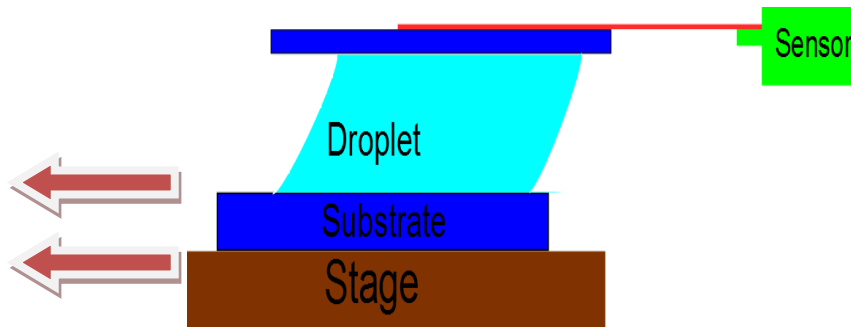


Figure 7: Stage Moves the Substrate under the Droplet and Causes Dragging Force

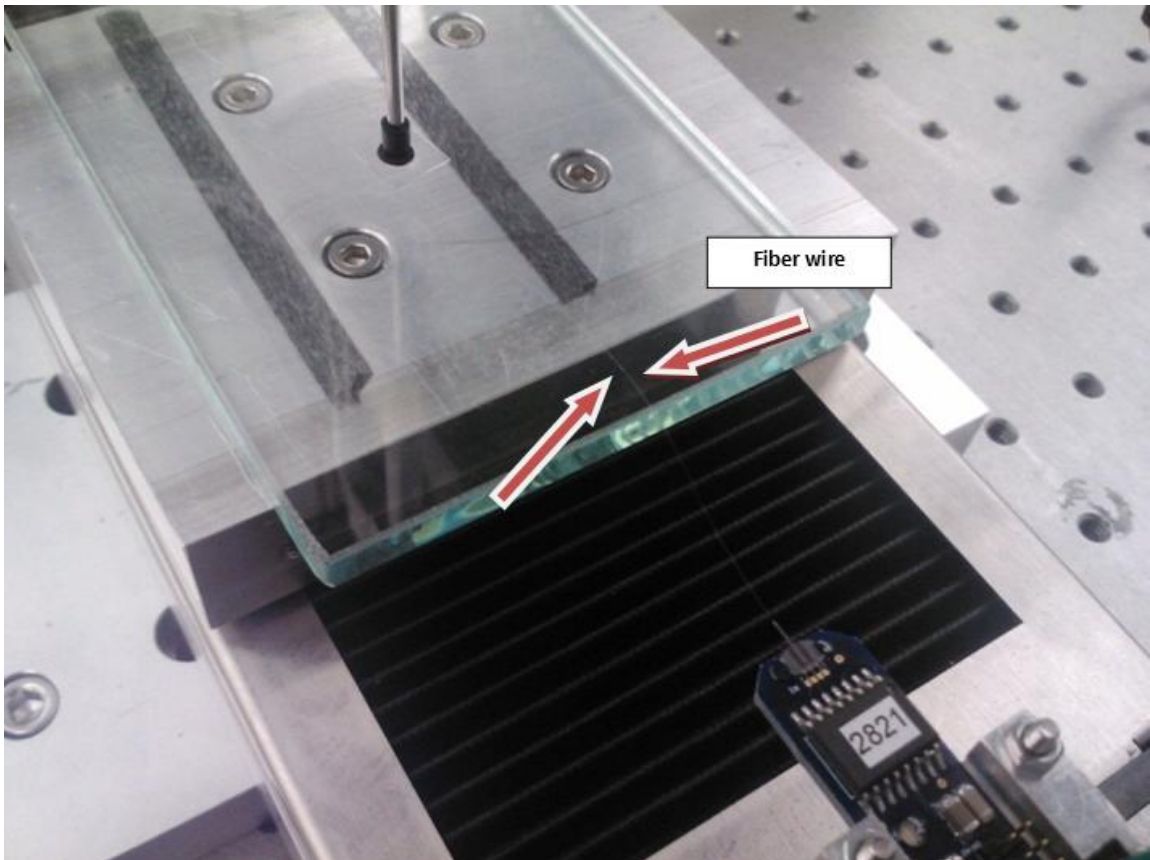


Figure 8: Fiber Wire is Attached to the Top Glass Plate and Sensor

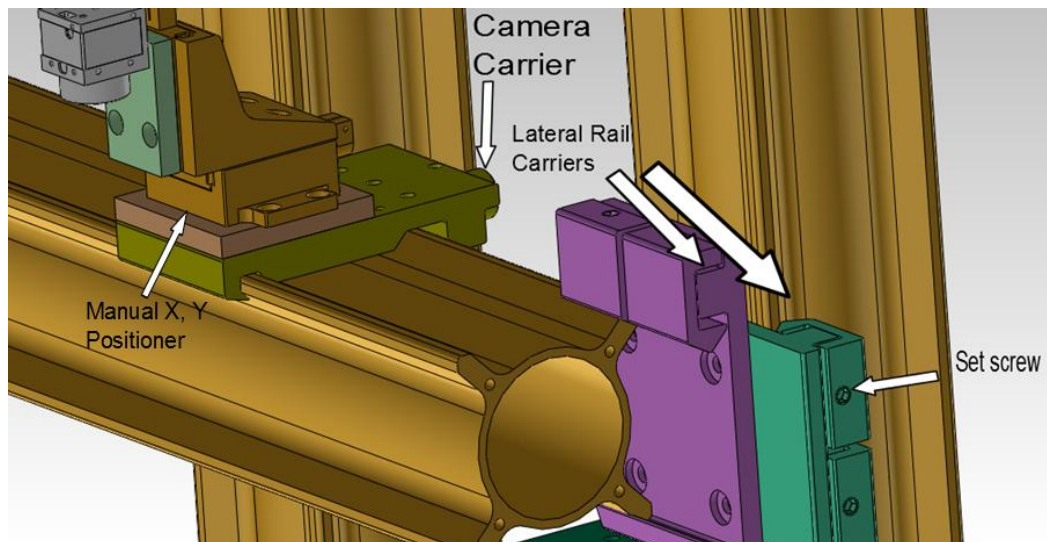


Figure 9: Carriers and X, Y Manual Positioner

The vibration isolation system consists of an air table and a stiff breadboard to reduce any vibration from the floor. The air table is adjustable by three pressure valves that are located under its heavy and stiff table. Also, the Breadboard has many thread holes on it that components can be installed on.

The visibility of the process and providing a clean room is another subject. Following that concern, a transparent box was designed to protect the test components from any dirt and environment noise, and a positive air flow was used to prevent the outer air from entering into the box while the operator keeps the windows open. A camera and lens also contribute to provide an observation system (Figure 10).

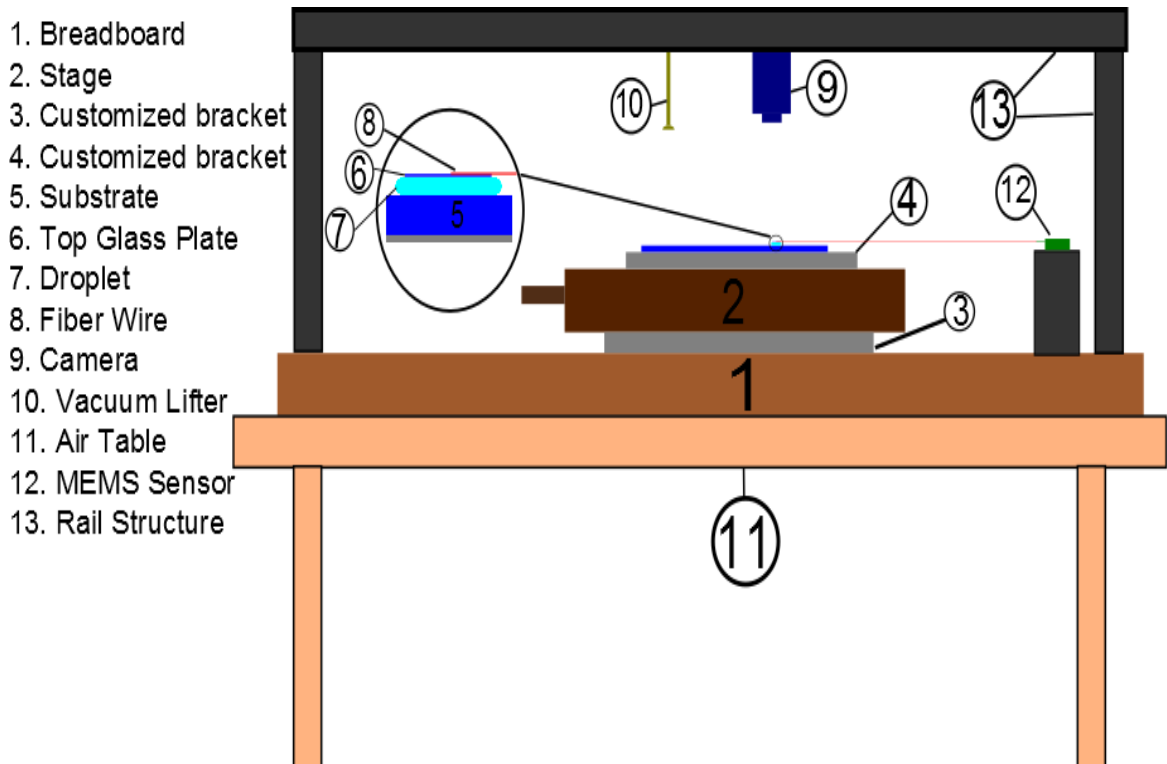


Figure 10: Design Concept

2.3 Linear Motion

A linear stage provides a motion that moves the attached hydrophobic substrate. In consequence of the static friction between the surface and the droplet, a horizontal load is applied to the droplet. This load is the droplet force and can be changed by changing the motion setting, or applied voltages in the case of electrowetting. The motion parameters are velocity, acceleration, deceleration, and traveling range. The stage is aligned with the sensor on X-axis. The linear stage in this design is a Newport product (UTS100CC) and has a traveling range of 100 mm. Its motion is produced by a ball bearing and some lead screw mechanisms. The DC motor in this stage arranges for very smooth travel with less noise, high acceleration, high velocity (of up to 40 mm/s) and a high resolution of 2000 counts per revolutions, which allows for highly accurate motion control. Another interesting note about this stage is the anti-backlash nuts that are used to prevent the stage from any errors. Full description of the stage is mentioned in Appendix A. [13] Respectively, because of the high sensitivity of the process, a stage with this level of accuracy is needed. By moving the stage the hydrophobic substrate which is attached to the stage moves.

2.4 Controller

In order for the stage to be able to move, an actuation force is required. In this application, it is important to have motion with different parameters. These

parameters include travel range, acceleration, deceleration and velocity. These parameters are determined by a controller. Esp301 series 3 axis motion is the controller model from Newport Co that we used. Programming of this controller is based on a language that comes as software with 100 commands. The most useful commands are acceleration (AC), deceleration (AG), absolute position (PA), relative position (PR) and velocity (VA). All the commands will be typed on the console and each line only accepts one command. Usually position command is the last order that should be input into the console and this causes the stage to start moving. The controller connects to a computer by a USB cable and has the ability to provide feedback of time vs. position as well as receiving commands directly from LABVIEW, so that after the data was collected we can find out the force value at each point of stage travel. For the safety the stage will stop traveling at the end point.

2.5 Measurement Force Sensor

The most important component in this machine is the measuring sensor. MEMS based sensors are capable of measuring small forces of up to 10000 μN . MEMS is an acronym for Micro Electro Mechanical Systems, which represents any device that is made of parts that can be as small as 100 micrometers. [14] The MEMS main body structure is mounted on polysilicon springs and enables the substrate to move in two directions. Around the main body there are many branches that are known as fingers. There are two fixed plates on the sides of each branch that

create a differential capacitor when the finger is moving back and forth. Labview is a software program that enables us to measure the differential capacitance of this process and converts it to force units. [15] The sensor that we used is one of Nanoscience Instrumental's Co products (FT-s100) with a measuring range of $\pm 100 \mu\text{N}$, a sensitivity of $50 \mu\text{N/V}$ (5 mg/V) and a resolution of $0.005 \mu\text{N}$ at 10Hz , which is a very high precision measuring device. The main issue of working with this device is its high physical sensitivity. The dimensions of the sensor tip is $3,000 \mu\text{m} \times 300 \mu\text{m} \times 50 \mu\text{m}$ and this means the tip can break easily with any transverse force that causes bending. This makes working with this tip very hard and handling should be avoided once the wire is attached to the tip and the top glass. Thus a precise lifter is needed to elevate the glass plate vertically after each test so that it can be prepared for the next round.

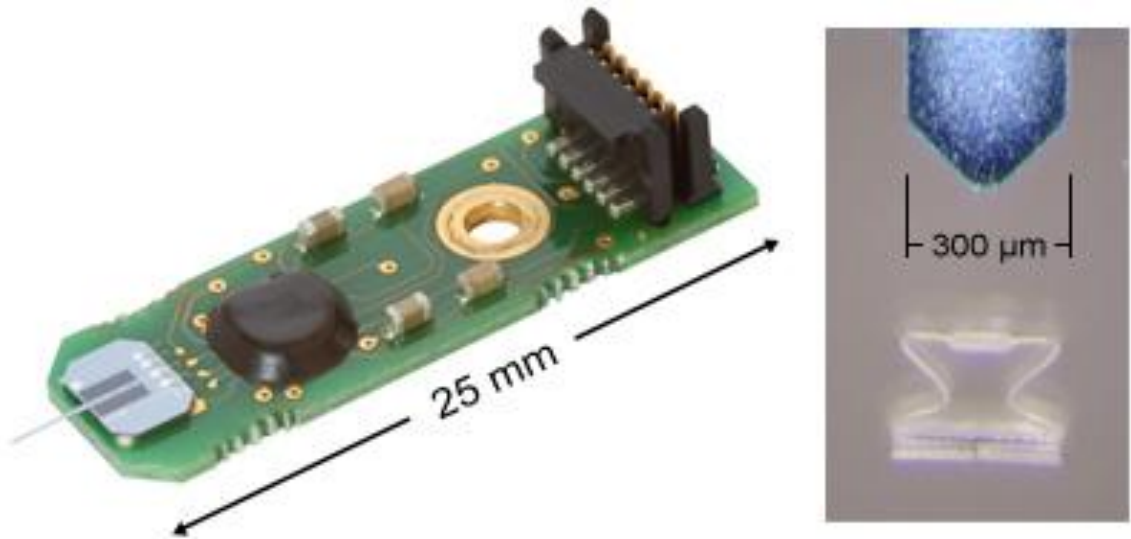


Figure 11: MEMS Sensor (Right) - Tip of Sensor (Left) (Picture is Taken from Nanoscience Co website, Used with Permission.)

2.6 Vibration Isolation

One important factor that can affect the results of the test is vibration. Vibrations can source from the floor, from other environmental noise, or from circulating air flow. In order to neutralize any physical vibrations, some techniques are applied which help to reduce any interference with the results.

2.6.1 Air Table

An air table is a product that is known as a vibration isolator and is made of a very rigid structure. A very heavy and stiff table rests on sealed leg isolators which expand and compress via a pneumatic mechanism. The diaphragm in the isolator plays a key role, and is essentially a very soft spring that applies a pressure that is supplied by the compressor.

Depending on the forces caused by vibration, the pressure will automatically change. There is also a check valve that protects the chamber in case of overdue pressure. The repeatability of the isolation supports can be up to $\pm 0.003''$ (0.07 mm). According to our research it is better to install high precision setups closer to the isolation supports, and the central area of the air table is the most stable area. [16] Different parts of a vibration isolation system are shown on Figure 12.

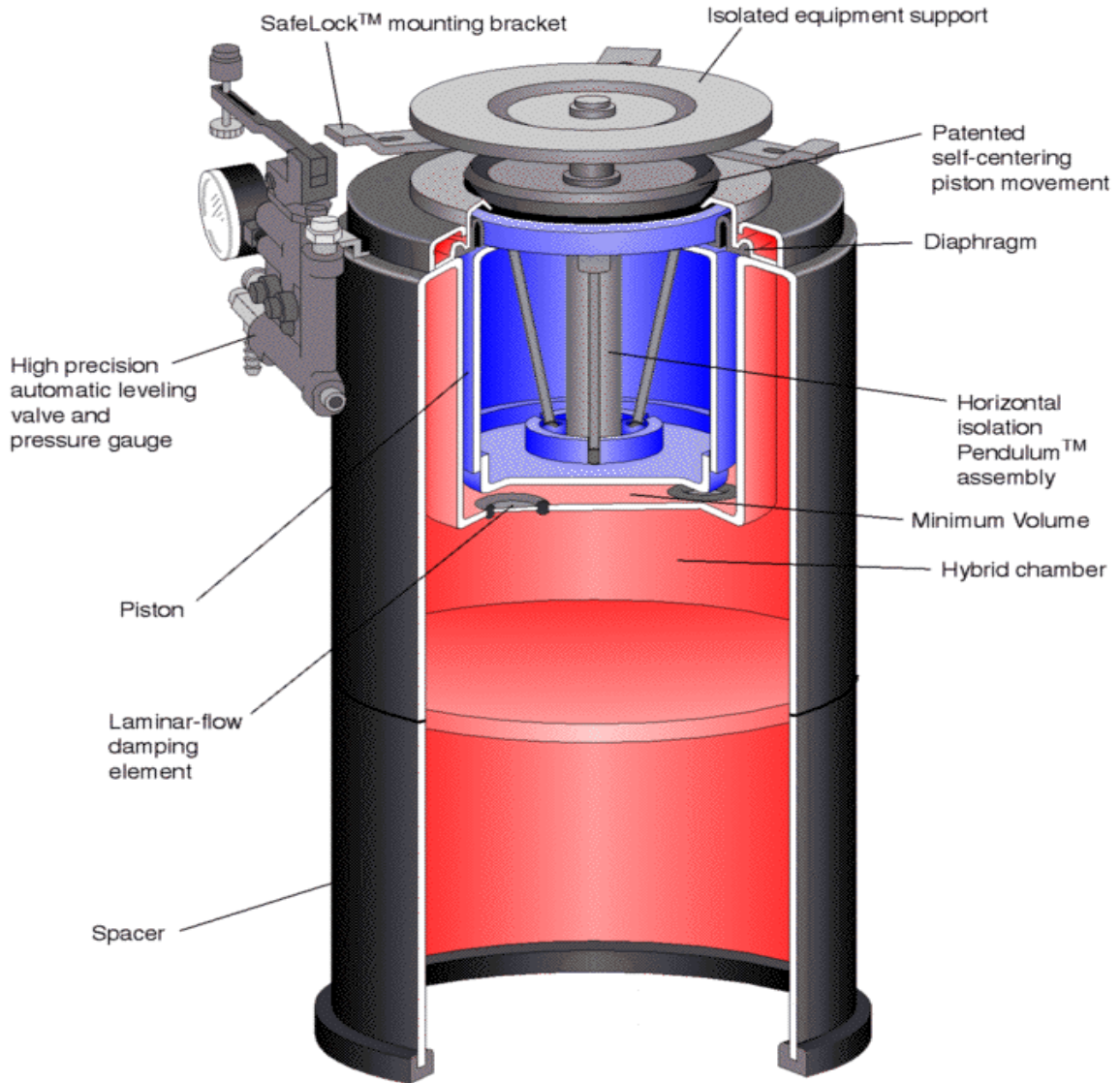


Figure 12: Isolation Support System (Used with Permission from Newport Co.)

2.6.2 Breadboard

The breadboard is one of the most important parts of each design because all of the components and setup are installed on it in order to be a referenced for data acquisition. Therefore it has to be very stable, and the material and structure must be very stiff. This is not only to prevent deformation due to its large

weight, but also is due to the ratio of its strength to its weight which is a concern.[17] Depending upon the application there are several different models that can be used. The breadboard that we used for our application is known as a sandwich. Two stiff stainless steel panels placed on each side of a honeycombed structure are tabbed with 1/4-20 thread and a 1" grid distance pattern to help the other components mount on the panels.

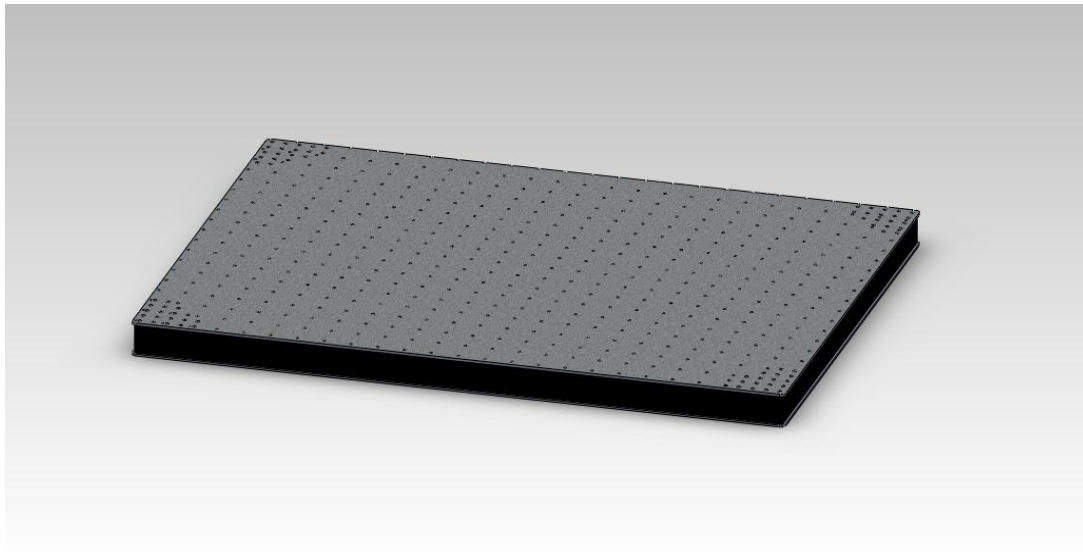


Figure 13: Sandwich Breadboard

2.7 Hydrophobic Substrate

A hydrophobic substrate is a surface with material properties that repels water and in this project it is a simple glass plate with a special coating. The coating process depends on the desired layer thickness and is different in terms of spinning speed, baking temperature and time. Coating starts by injecting CYTOP on $\frac{3}{4}$ of the glass surface very slowly (30 $\mu\text{l/hr}$). Then the glass spins for 500 RPM for 5 seconds and after that increases to 2000 RPM for 20 seconds to

spread CYTOP evenly on the surface. Throughout the next 5 seconds the spinning will decrease until it stops and it is ready for pre bake. The coating will then rest on a hot plate for the next 90 seconds at a temperature of 100°. Then the coated glass is placed in a 200° oven for 1 hour. [18] After the process of coating the hydrophobic glass attaches on the Stage. Some simple glass plates were used underneath the coated substrate to align with the tip of the sensor.

2.8 Vacuum Lifter System

Each time the stage moves the substrate under the droplet causes the top glass plate to drag the tip of sensor, but the sensitivity of the sensor is high and so the tip can break very easily. This type of sensor is designed to drag the tip but not to put pressure on it. Also, the fiber wire is bonded to the tip and the top glass, and this dragging force can occur by moving the substrate on one direction. It should be noted that substrate cannot move on reverse direction due to the pushing force that it causes. That means after each test round, the top glass plate should be position fixed and return the substrate to initial position. This creates a challenge that how to pick up a very thin glass plate without causing damage to the sensor and the other components. One concept was to vertically bond a very thin tube on the glass plate and grab it with a fiber-chuck that is mounted on a three axis micro positioner. There were two problems with this idea that prevented it from being practical: firstly, adding a tube on the glass plate would increase weight of the top glass plate which is supposed to be

negligible. Secondly, by girthing the fiber, a torque force is applied to the glass plate and causes the plate to rotate and again this could result in breaking the tip of the sensor. The next idea was to use a negative air flow that mounts on the same manual positioner in order to adjust it slowly and coordinate it as close as possible to the glass plate to prevent any shock to the sensor. The vacuum system consists of 2 valves; one use for pressure control and the other one use for turning the air flow on and off, as well as a 5 mm hose, a 2 mm needle and a 0.08" cup.

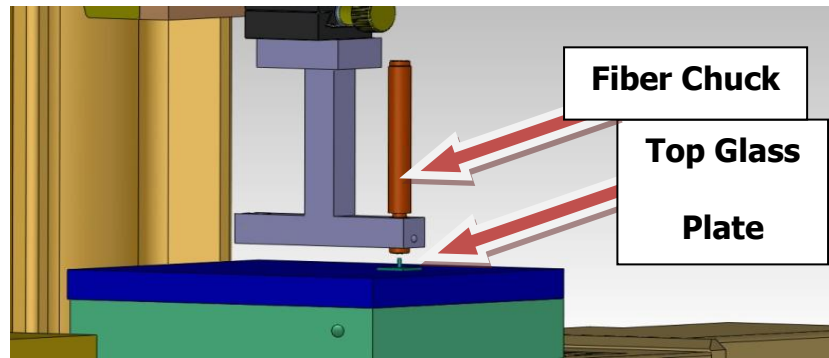


Figure 14: Picking up the Top Glass Plate with Fiber Chuck in a 3d Model

The advantages of vacuum lifting are that no more physical lifting process is involved and moreover there is no need to coordinate the needle at the exact position. It should be noted that high pressure might cause the glass to stick to the cup and thus would not release when cutting the pressure. The micro positioner that is used to mount the needle is a Newport product and the 1" hole on it helps to place the needle in it and fix it by a set screw.



Figure 15: Vacuum Lifter

2.9 Structure

The Breadboard is referenced to the other components. As a result the main components such as the stage and the structure are installed on it. The structure consists of two base plates that connect four side rails to the breadboard, three rails with 0.5 m length, two right angle joint carriers with through holes, two right angle joint carriers with taped holes and two right angle joint carriers with captive fastener screws that help to mount and remove the carriers from the rails quickly. There are also some customized parts that are required to connect different components such as the camera and the micro positioner to the carriers. The four reinforcement ribs on the rail are the features that guide the angle joints of the carriers. The extrusion manufacturing process provides easy traveling for the carriers on a very smooth surface with less friction. All the structure parts are made of aluminum which makes them light weight. Due to

the few adjustments that apply to the height of the structure, the right angles joint carriers have the option to be positioned on the rail by two set screws.

2.10 Observation

It is important to monitor the process visually. Because of this, pictures and videos can be helpful to document the study. In addition, depending on the volume of the droplet, the camera helps to align the top glass plate to the tip of the sensor. The camera can mount on a rail carrier and travel across the testing area while recording picture/video vertically or it can be placed on a bracket on the breadboard and have a side vision. The camera is mounted on the same micro positioner as the vacuum lifter for small adjustment. There is a concern for the focal length of the camera, as it has to be far enough to provide the best picture quality. The camera (EO-0413M 1/3") is an Edmundoptic Co product with a resolution of 752 x 480. There is a 1/4-20 thread on this camera to use for mounting. The minimum focal length of a lens that can have field of view of 1"x1" is 25 cm and respectively, the distance between the droplet and the camera should be more than the focal length at least. Depending on the needs, different lenses can be used. Focal length lenses can optimize the vision performance while having high durability and the compact design was the criterion used to be chosen in our application.

2.11 Conclusion

After understanding the functionality of the test and the results we are looking for, the concept of design was figured. First, the basic design was configured by SOLIDWORKS to simulate the design and model the required principals of the test. Then the design was developed by applying some techniques to reduce interference on the data, such as the vibration isolation system. Some equipment was added to the machine in order to set the initial preparation of the test after each round. A camera was added to the machine to record desired videos and pictures. After the prototype was completed and all the issues and problems solved, all the devices were purchased and all the required customized parts were fabricated and then assembled together. In picture 13 and 14 different parts of the machine are addressed in the final design.

Table 1: Component List of Measurement Machine

Item Number	Component	Item Number	Component
1	Camera	6	Vacuum lifter
2	Micro positioner	7	Hydrophobic Substrate
3	Structure	8	Stage
4	Right angle carrier	9	Breadboard
5	MEMS Sensor	10	Air table

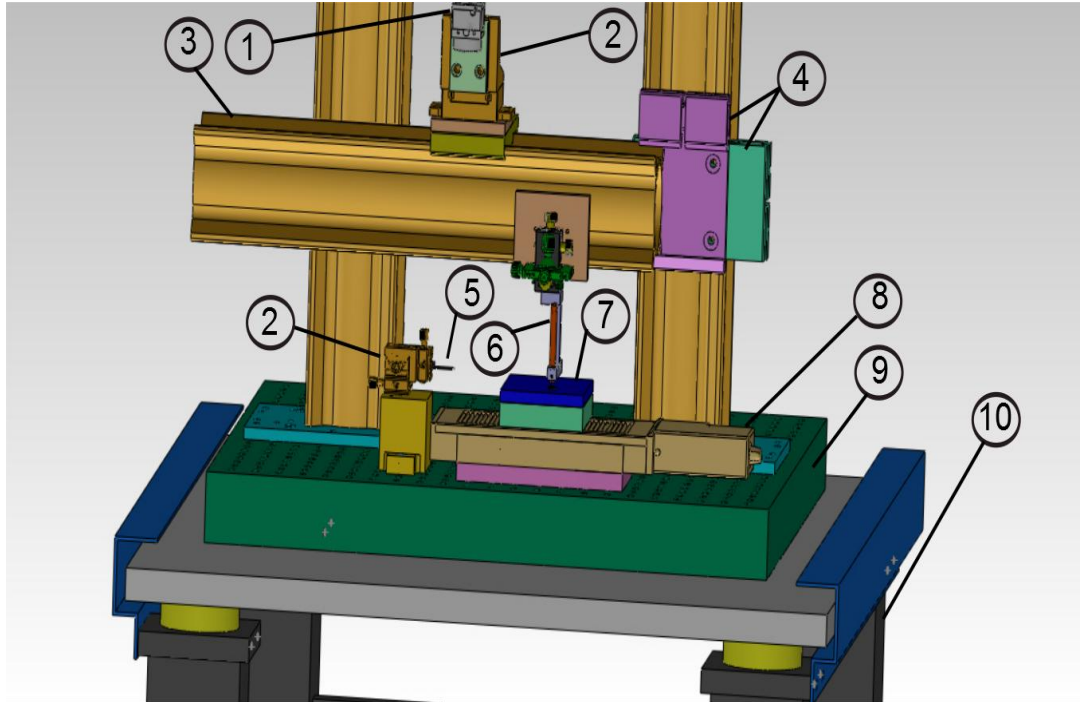


Figure 16: Design Prototype

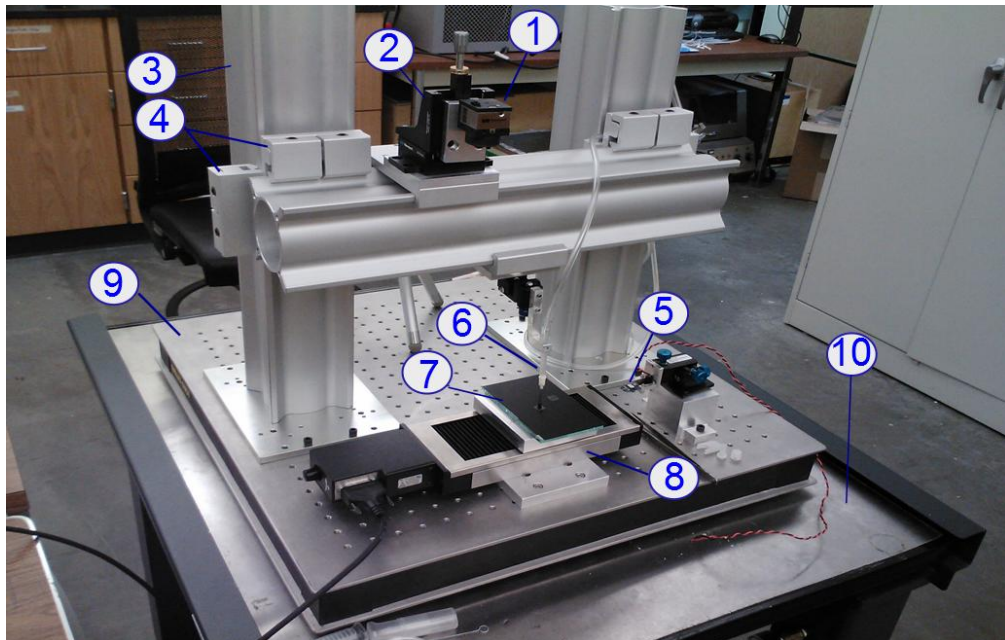


Figure 17: Assembled Machine

CHAPTER 3: DESIGN OF CLEAN BOX

Through this set of contents the importance use of an enclosure box will be discussed and how design concept was developed. Then in details each component of the box will be argued over the usage and challenges of being chosen. This section of the project was assisted by Timo Marschke.

3.1 Concept

The idea of using a box came once we figured out how much change on the data can occur from different environments while running the test. Due to the small scale of our force measurements anything small can make the results incorrect. These can be caused by air flow, dirt, noise vibration or any accidental touch. Following that concept, use of environment isolation was necessary. A box with enough stiffness to minimize noise transmission and air flow was needed for this design.

On the other hand this box is supposed to be transparent enough to enable us to see the test operation. To be able to see the operation is important not only because of the research study but in case something goes bad. The challenge was to make the box isolated from the air in the environment in order to keep

the testing area clean. Also, during set up there needed to be a way to prevent the outer air from getting in. Thus an air flow system was considered that starts working when the access areas are open. The wall sheets of the box are attached to a structure that stands on the floor to give more stiffness to the box so that it can withstand any external force on it.

3.2 Transparent Box

The concept of the box was based on a clean experimental space to be big enough to contain all the components above the air table. Additionally, the transparency of the box is important, as it is crucial to have enough light inside the box to observe the process. Due to the fact that the test process needs to be repeatable and constantly rearranged, having easy access to the test setup is an important concern. Along these lines the material we used for the wall sheets are acrylics that are transparent. Using an acrylic sheet allows us to do modifications on it without causing the sheet to break. Two sheets with dimensions of 33.7" x 32" x 0.5" are located on the front and back sides of the box, along with a 13" x 8" x 0.25" window on the front side, in order for the operator to have easy access to the setup. Side wall dimensions are 37.8" x 32" x 0.5" with another window on the right sheet with the same size as the other window. The top side of the box is designed specifically for air flow entrance. It is made out of wood and consists of a simple sheet with an 11" x 11" square hole on it. There is another box on top of the wood sheet which is designed for the air filter. This

box is also made out of wood with dimensions of 16" x 16" x 4" with a thickness of 0.5" that is secured by two clips on the sides.

There are some holes with diameters of 6.8 cm set around each wall sheet at distances of 5" in order to attach the wall sheet to a structure and enhance the stiffness of the wall sheets.

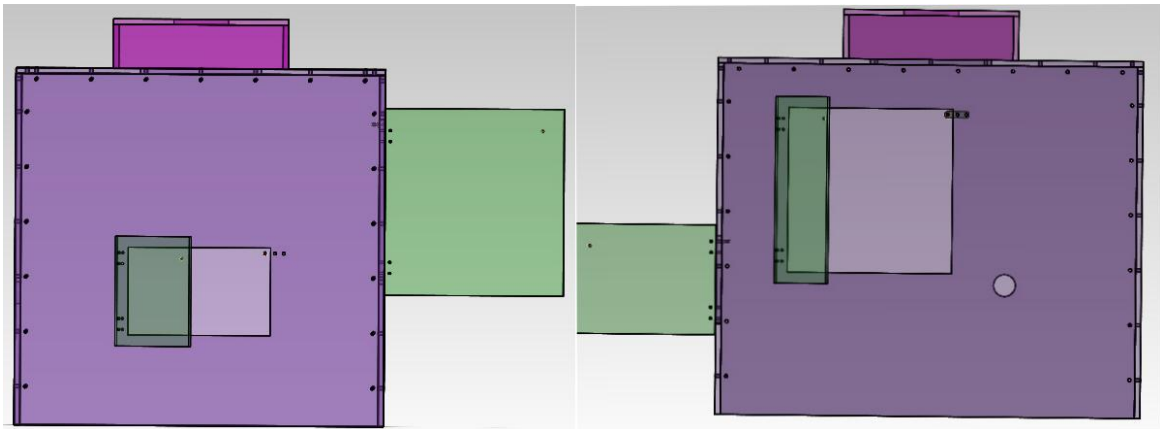


Figure 18: Front Box View Prototype (Left) - Right Box View Prototype (Right)

3.3 Enclosure Structure

The purpose of this structure is to support the wall sheets and offers a separated support from the platform to the vibration isolation system. Hence any external disturbance will not affect the measurement process. It is important for the transparent box to be stiff enough to withstand any internal/external forces because the box is actually the protector of our test components and test results. In order to increase the stiffness of the box, the wall sheets are attached at

several points to a metal structure. The structure should be stiff enough to support the acrylic sheets. This structure is shaped in T-slots and manufactured by extrusion method. They are like a block with constant slots alongside them on each four sides. These slots help to place a nut into them, slide it into position, and attach a bolt to it. With this light weight precision product you can create the structure, safe guards and a workstation without being worried about stresses and bulking. Extrusions of these structures are done to convert raw material to finished product. The advantages of using such a product are its light weight, stiffness, anodized finish, it does not require welding or painting, it is corrosion resistant and working with it is fast and easy. In order to enhance the structure, a 12 mm corner bracket is used on each internal corner. As mentioned earlier, there are some holes on the left, right and top sections of the acrylic sheets that are used to attach the structure to them. There are four T-slots with dimensions of 1" x 1" x 55.5" that are the legs of the structure. Also there are shorter lengths T-slots with the size of 1" x 1" on the section and with lengths of 32.7", 30.6" and 35.72" that are located between the standing legs. There is also a 22.5 mm gap between the box and measuring machine structure to prevent vibration transferring from the box to the measurement machine. Assembling all the box components were done by Timo Marschke and Qi NI.

Table 2: The Box Components List

Item Number	Component	Item Number	Component
1	Filter Vent	6	Side T-slot
2	Inside Corner Bracket	7	Standing T-slot
3	Front Window	8	Up Front T-slot
4	Side Window	9	Cable Vent
5	Down Front T-slot	10	Acrylic Sheet

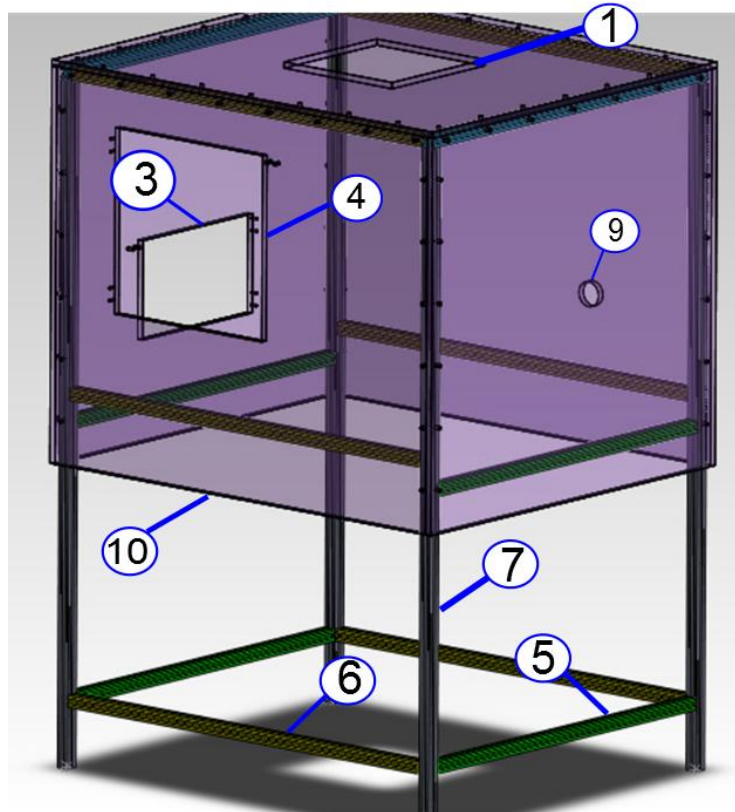


Figure 19: Structure Prototype

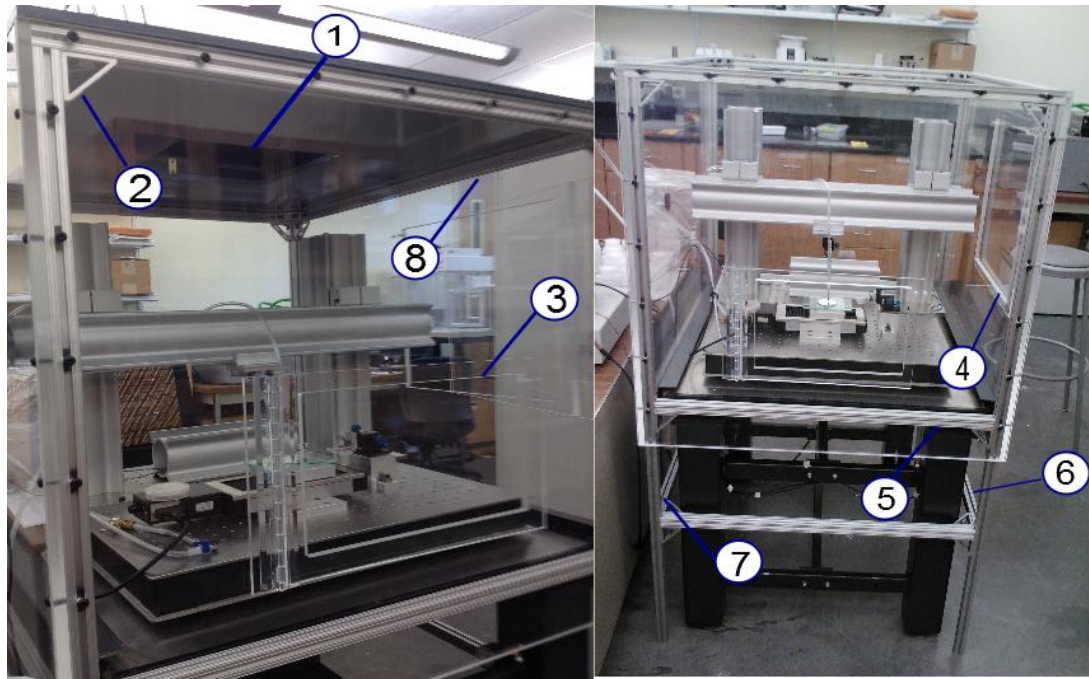


Figure 20: Assembled Box

3.4 Clean Room

Any small interference on the test process might end up with the wrong results. As mentioned earlier in previous chapters, the isolation box and vibration isolation system are used to increase the accuracy of our measurement. There is small gap between wall sheets and air table edges. However, the internal space of the box keeps the experiment components clean. Another difficulty is in how to keep the internal box isolated from pollution and dirt while the windows are open and the operator is arranging the setup.

3.4.1 Positive Air Flow

After running each test and collecting data, it is necessary to pick up the top glass plate and return the stage to its original position. To prevent the environment air and dirt from entering the box, a positive air flow is needed which is filtered and clean. The fan in our application is "Soler & Palau In-Line Fan TD-250" with a duct size of 10", can work in 2 speeds, and can induce air flow between 475 to 754 CFM. It should be noted that filters that are applied in the system cause to drop the pressure. (Research for the fan and filter was done by Timo Marschke). That means with neglecting the resistance along the duct and through the filters, the air speed from one window would be 1.91 m/s at its highest speed. This speed is perfect for our application because higher air flow might move the top glass and end up breaking the tip of the sensor. On the other hand, less air flow would let external air and dirt get into the box. An air filter with dimensions of 12.5" x 2.5" x 13" is inserted into the wood box and used to clean the fan's air flow. The other advantage of using an air filter is that air flow does not pass through in certain sections and the filter spreads the flow equally through the square hole. By attaching some Confined-Space Conical Compression Springs to the filter box we can then clamp up the filter. The first idea we used for starting the fan working was based on an automatic mechanism. There is a switch that is called "push to break" that is used to keep the electric circuit disconnected as long as the button is pressed. Once the button releases the circuit will be connected and the fan starts working. By

mounting this switch on the wall sheet, the fan starts running when the window opens. The problem with this idea is that it may take awhile for an air current to start inside the box. As a result, a manual switch was used in order to turn the fan on a few seconds before opening the window. Also, a one-way valve can be added on one of the wall sheets to release any extra air pressure in case the operator forgets to shut the fan off. The other components that are involved with positive air flow are a 10" duct and clamps to secure the duct on the wood box and the fan. A 2" hole on the left side of the box lets the cables enter and connect to internal components.

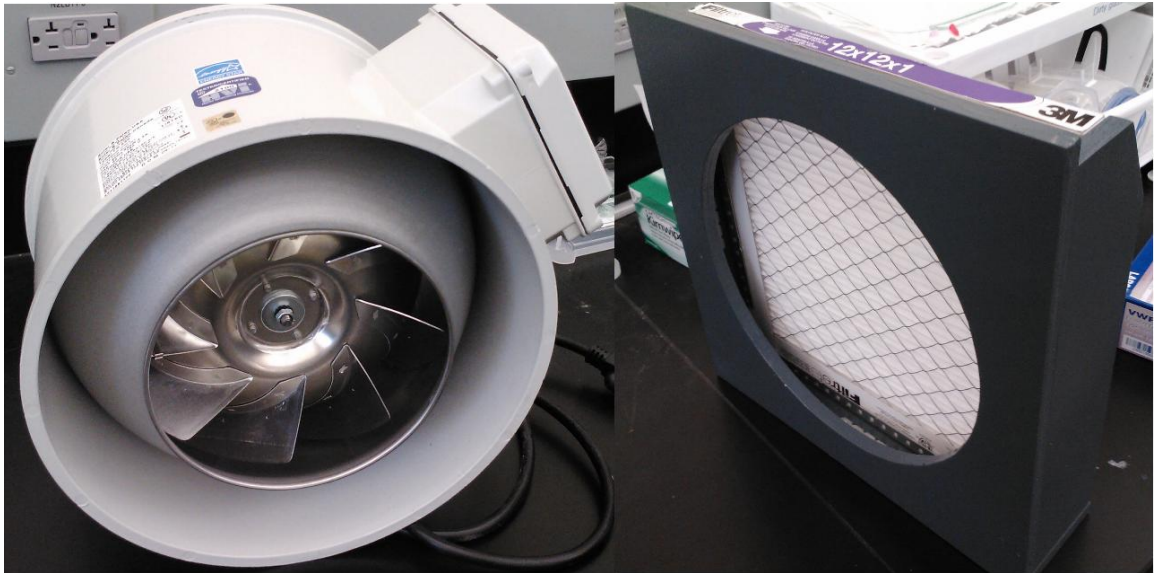


Figure 21: Fan (Left) Filter in the Customized Box (Right)

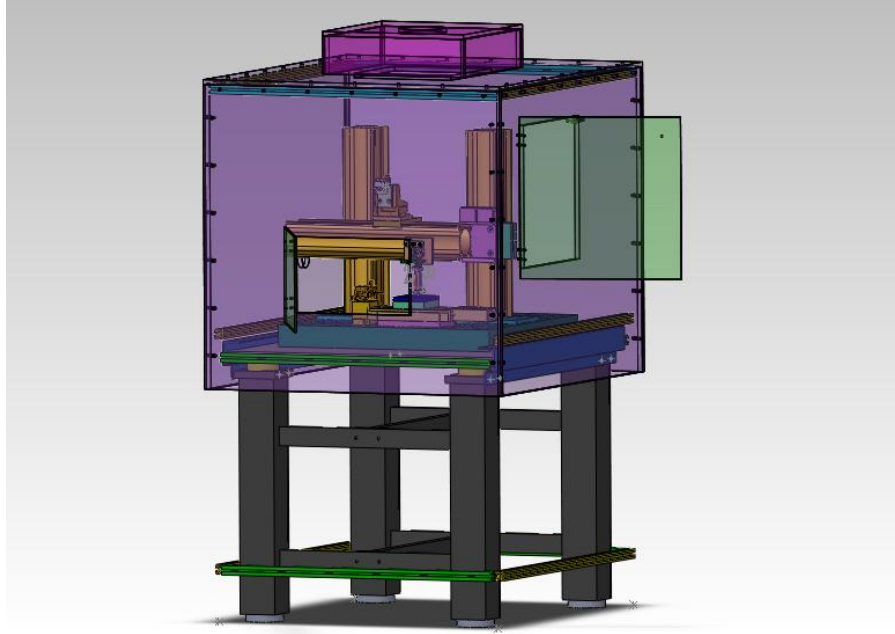


Figure 22: Isometric View of the Complete Machine Prototype

CHAPTER 4: PROCESS

There are certain concerns to prepare the setups for each test process and configure it for next round. First the process will be explained and what steps are required to prepare the test process. Then it continues how data is being collected and how the contact line friction force can be changed by defining the motion parameters. Finally the parameters that are effective in the test process will be discussed.

4.1 Process of Measurement

In order to measure the actuation force of any fluid droplet, there are instructions that need to be followed. These instructions apply to the substrate, the bonding wire to the sensor, the coordination of the sensor and the position of the droplet on the substrate, the running of the stage with different acceleration and velocity, and at the end preparing the setup for the next testing round.

4.1.1 Preparation

Depending on the application, different components with a variety of material properties can be used on the test. In initial experiments we used a hydrophobic

substrate with CYTOP coating on a glass plate. The substrate must be secured on top of the stage in order to move with the stage and to let the droplet slip on it. Due to the high sensitivity of the sensor, the fiber wire can only be attached to the tip by bonding. It also should be noted that the top glass plate should be level with the tip of sensor due the ability of the sensor to measure only tensile force. Applying any transverse or bending forces damages the sensor. Thus, the wire bonds to the top of the tip and top center of the 9 x 9 mm glass plate. The next step would be to add the droplet. By using a pipette tip, the fluid is deposited on the substrate in any amount of volume in micro scale. The glass plate should be positioned as close as possible to the droplet with the micro positioner that the vacuum needle is mounted on. Then by disconnecting the negative air flow the glass plate would be released and would rest on the droplet. It should be noted that during set up positive air flow inside the transparent box is active and after closing the windows the fan should be shut down. At this point the test is ready to run and collect data. The controller has software that receives orders and can be programmed using commands. There is also a tab for jogging the stage which is useful for quick traveling regardless of the range and accuracy or in case the stage reaches the encoder switch point when this option needs to be used.

4.1.2 Programming

Every time before running the test the motion setting should be checked. Table commands are used to set up the stage configuration and start a movement. Figure 23 shows the way that is recommended to enter the commands in the terminal window. The "PA" command means the stage travels in respect to a coordinate point which is defined by the "GG" command. On the other hand, the "PR" command sends an order to the stage to travel in respect to its current position. It should be noted that before each command the number of the axis should be addressed. However, it is suggested to program the stage and send the commands by Labview, which is faster, easier, and avoids having accidental mistakes in typing commands. Also, it enables the position of the stage to be recorded and synchronized along with its velocity and measuring forces.

Table 3: Controlling Commands

Command	Function
AG	Deceleration
AC	Acceleration
VA	Velocity
PA	Travel Range Based on Absolute Position
PR	Travel Range Based on Related Position

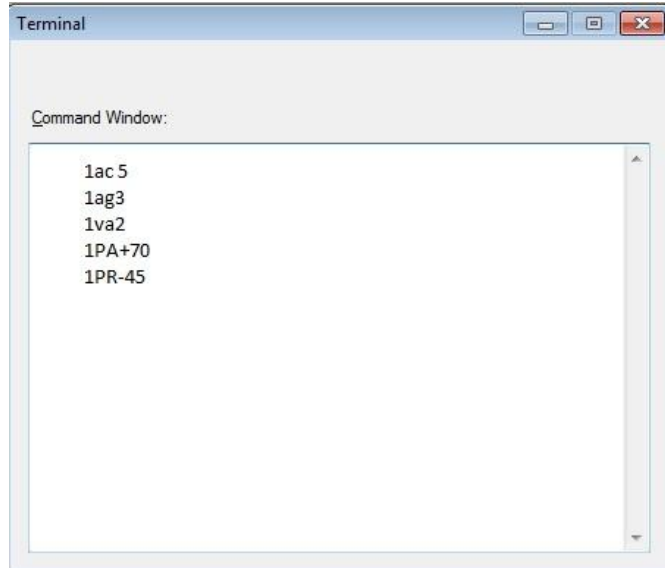


Figure 23: Programming the Stage

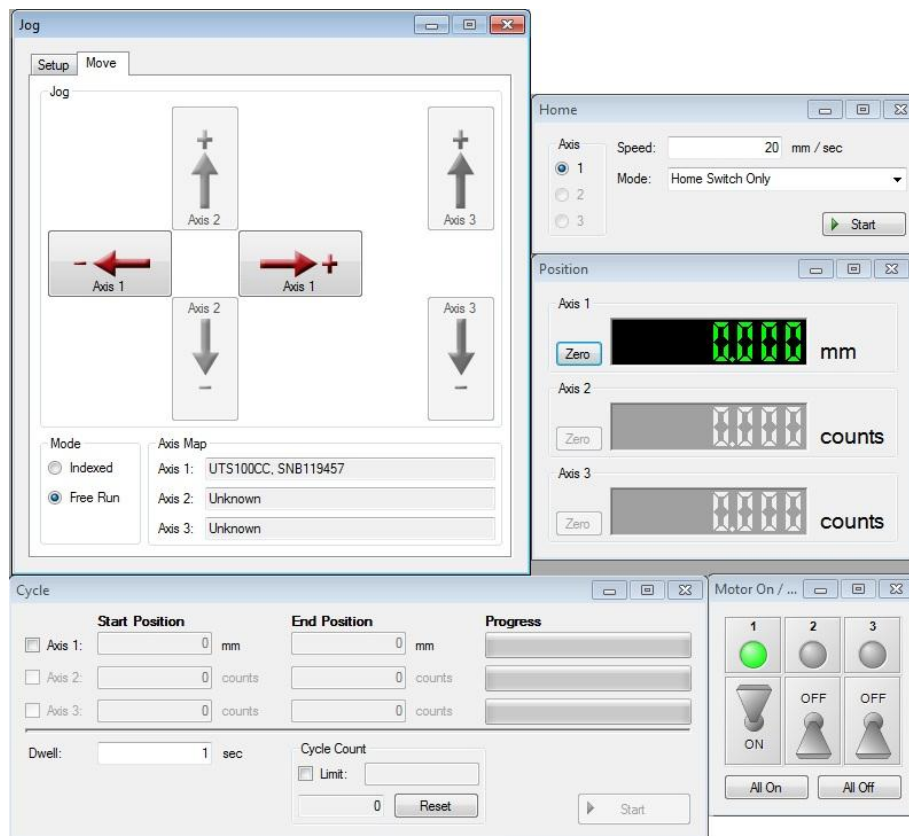


Figure 24: Programming Stage with Jogging Window

The other way of moving the stage is by using the jogging window, which is a quicker method. By this option, the stage can travel along the linear axis as a free run just by holding the mouse click.

4.2 Formula and Calculations

The following physics equations are related to the subject of kinematic motion and can be used to calculate the position, velocity, time, acceleration, deceleration and displacement of the process. The principals of the following equations contribute to figure 25.

$$\text{Total Travel Distance} \quad x_0 = v_0(t_0 - t_a) \quad (5)$$

$$\text{Constant Velocity Travel Time} \quad t_b = t_0 - (2 * t_a) \quad (6)$$

$$\text{Maximum Speed} \quad v_0 = \frac{x_0}{t_a} \quad (7)$$

$$\text{Deceleration/Acceleration Time} \quad t_a = t_0 - \left(\frac{x_0}{v_0}\right) \quad (8)$$

$$\text{Constant Velocity Travel Time} \quad x_b = v_0 - t_b \quad (9)$$

$$\text{Deceleration/Acceleration Travel Distance} \quad x_a = \frac{(v_0 * t_a)}{2} \quad (10)$$

$$\text{Total Travel Time} \quad t_0 = t_a - \left(\frac{x_0}{v_0}\right) \quad (11)$$

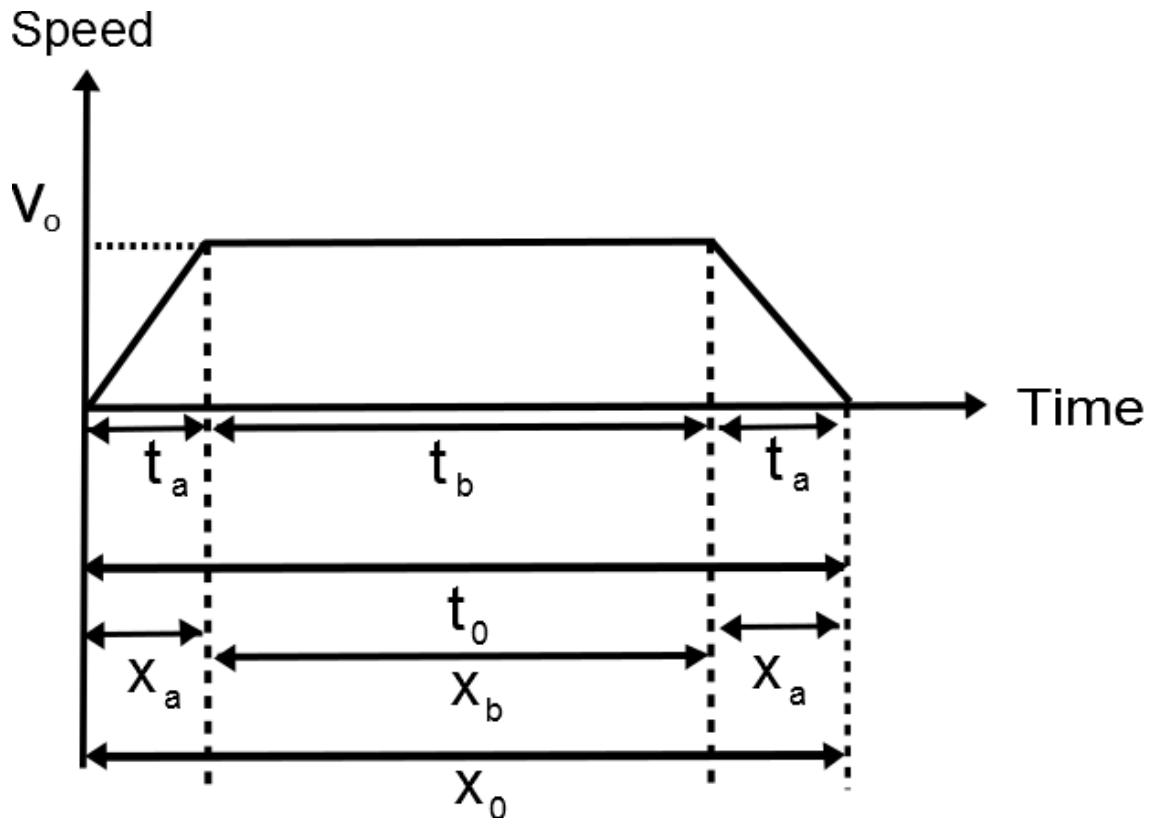


Figure 25: Velocity-Time Diagram

4.3 Test Configurations

In this set of experiments there are some configurations that are able to be changed.

4.3.1 The Interfacial Tensions Between Liquid and Vapor

The Substrate material properties define this coefficient value and according to The Young–Dupré equation (Thomas Young 1805, Lewis Dupré 1855) if the spreading parameter of a droplet is positive, fluid is wetting. On the other hand when this parameter is negative, fluid has little wetting. By having different

coating on the substrate, the interfacial tensions between liquid and vapor changes (γ_{SV}) and affects the slipping condition of the droplet.

$$S = \gamma_{SV} - (\gamma_{LV} + \gamma_{SL}) \quad (12)$$

4.3.2 Droplet

The actuation force of a variety of types of droplets with different viscosity can be measured under optional volume control. However, very low volume under influence of shear force causes the glass plate to be tilted. Large volume encounter same problem and it might result from large torque that drives from the larger distance that top glass plate has due the higher volume of droplet. If this happens while it is close to the substrate and there is any interaction between them, this can result in scratching on the substrate coating. Moreover, having too much volume in the droplet might cause it to not stick to the top glass plate while the substrate is moving. The possibility of this kind of deflection increases if the stage moves with high acceleration.

4.3.3 Motion

The Stage can move with a minimum velocity of 10 $\mu\text{m/s}$ with almost 6% stability. The Graph in figure 26 is provided by Newport Co following our request to estimate the lowest speed that the stage can move. Usually the minimum acceleration is around 4X the speed, which means the slowest speed increment

is around 40 m/s . Following that discussion the stage can move between 10 $\mu m/s$ and 40 mm/s on a linear axis.

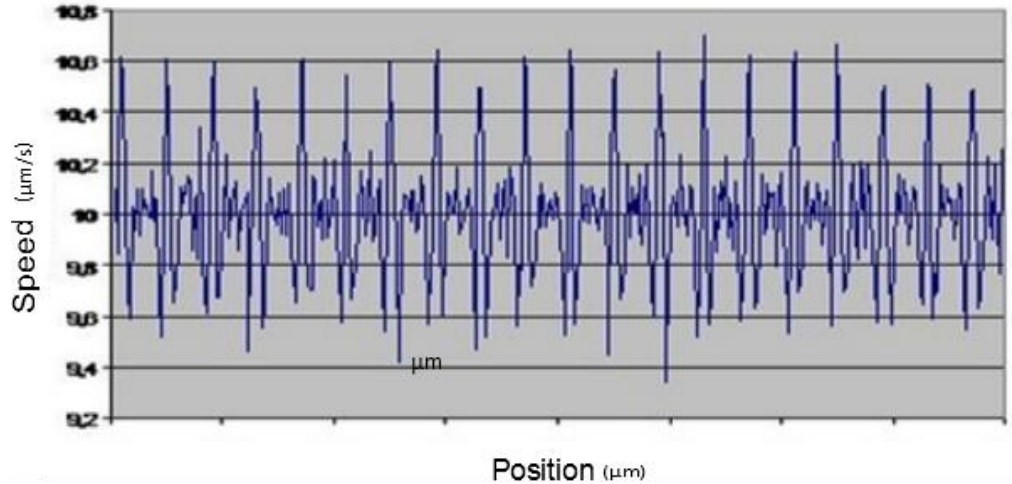


Figure 26: Speed Stability at 10 $\mu m/s$ – Sampling 50 Hz (Used with Permission from Newport Co.)

4.4 Programming

Programming the stages with Hysitron's machine is harder and more time consuming due to software that is provided that has a lot of problems as it locks up if the stage passes the limited range and needs some manual adjustment to fix it. Moreover, the machine is made mainly to measure the hardness of the thin films and the sensor tip is designed to have a vertical movement direction.

Although our machine is using the same stage it is also able to be synchronized to LABVIEW software.

CHAPTER 5: RESULTS

Chapter 5 helps to compare traditional method of measuring the contact line hysteresis with the direct measuring of contact line friction. Then a similar commercial machine will be compared to manufactured design as aspects of accuracy, price, user friendly and data results.

5.1 Theoretical Measurement vs. Direct Measurement

In chapter one different methods of measuring the water droplet contact angle were mentioned. Contact angles can be used to calculate the hysteresis force. However, with a new method we can directly measure pinning force and study the differences or similarities between them. Table 4 shows the contacting angles that were measured with captive needle. The depositing rate of the water droplet is 5 $\mu\text{l/s}$, and after the first deposit, the needle should be very close to the substrate and located in the center of the droplet. The process of adding more droplets continues till the droplet reaches its maximum contacting angle which is its advancing angle. That means the droplet shape will change suddenly. Reversing this process defines the receding angle before the droplet moves. [19] The contact angles that were measured by tilting are mentioned in table 5. In this method certain volume of the droplet adds on the hydrophobic substrate and

by using a manual fixture, different angles applies to the substrate. A camera records the ending angles before the droplet moves. As mentioned in section 1.3.2 advancing and receding angles were defined. The contact angles can be plugged into formula (3) and hysteresis force can be calculated. The water/air surface tension coefficient is considered as 72 mN/m. [19]

Table 4: Measuring the Advancing and Receding Contact Angle with Captive Needle Method (Table from [19])

Advancing (Degs)		Receding (Degs)	
115	112.9	98.6	99.5
115	116.4	101.9	101.4
114.6	114.8	98.6	97.9
114.7	115.7	98.6	97.9
114.5	114.9	99.4	99.1
Force/Unit Length (mN/m)		18.9	
Std.Dev		2	

Table 5: Measuring the Advancing and Receding Contact Angle with Tilting Method (Table from [19])

Volume	Advancing (Degs)		Receding (Degs)	
10	117.7	114.5	106.2	96.8
	114.5	116.0	100.3	109.4
15	115.9	115.5	97.4	108.9
	120.4	117.5	105.6	99.0
115.6	117.0	117.8	105.9	103.2
	115.6	116.9	106.6	103.9
25	114.3	115.8	102.4	104.4
	114.4	116.1	100.6	107.2
Force/unit length (mN/m)		15		
Average/Std.Dev	116.2/1.61		103.6/3.88	

Table 6: Measuring the Contact Friction Force with Direct Method (Table from [19])

Acceleration (mm/s ²)	Max Force (μN)				Force/unit length (mN/m)	
	42 μl	Std	63 μl	Std	42 μl	63 μl
0.3	X	X	91.91	5.9	X	10.21
0.5	X	X	91.4	23.5	X	10.16
1	97.4	8.47	103.9	17.4	10.83	11.55
2	112.9	21.3	109.1	21.1	12.74	13.73
3	114.7	8.93	123.6	25.1	12.74	13.73
6	120.5	7.58	132.5	13	13.39	14.72
9	125.2	1.39	128.5	15	13.91	14.27

In the direct measurement method contacting angle is not a concern and the actuation force will be measured directly. The tests were performed under different principals, namely velocity and acceleration. In the following graph (Figure 27), friction force between a water droplet with a volume of 41 μl and a hydrophobic surface was measured. In this set of tests, the stage runs with velocities of 1 and 2 mm/s, as well as accelerations of 0.3, 2, 4, 5 and 6 mm/s. According to the graph the force increases tremendously in the first few micro meters and it grows even more by running the motion with higher accelerations. By comparing the results from direct measurement with traditional dynamic methods we notice that the data is close together and this could mean that contact friction force and hysteresis force could be similar. The differences between traditional measurement and direct measurement might come from

environmental influences like air pollution, mechanical noise or electrical noise. Table 6 also shows that by increasing the motion's acceleration, steady state velocity decreases and the standard deviation of the force increases. Thus it is suggested that by decreasing the motion acceleration we can approach traditional measurement data to direct measurement data.[19]

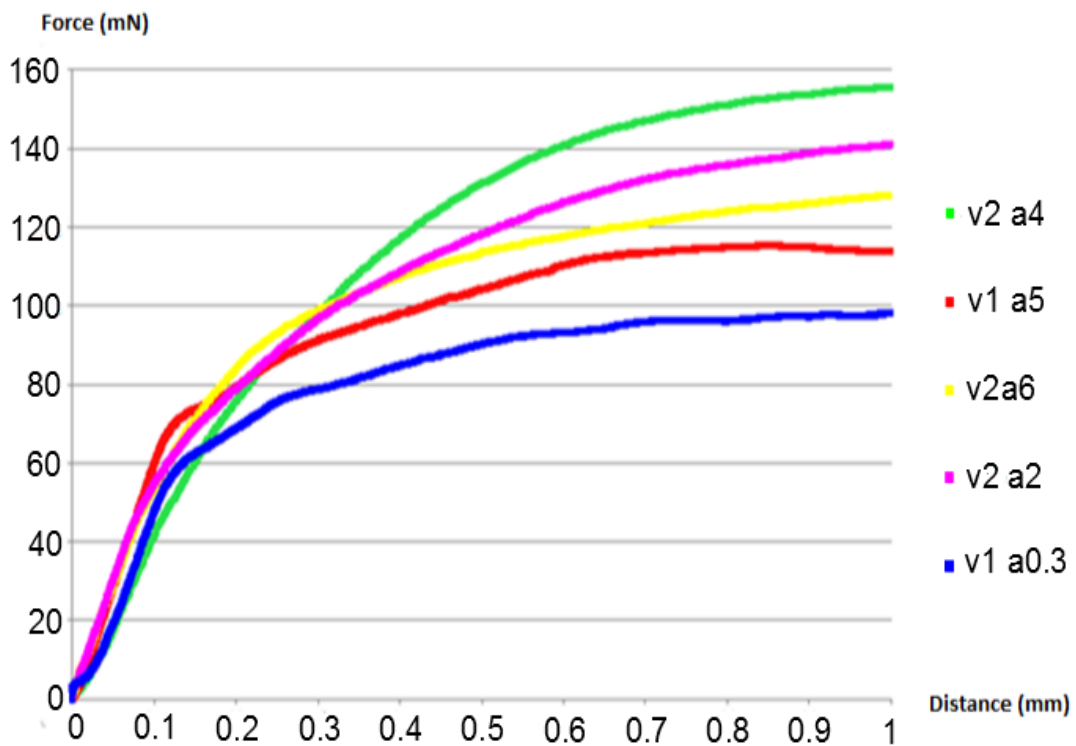


Figure 27: Force (N) vs. Distance (mm) on Volume 41 μ l by Customized Machine [19]

5.2 Comparison

Hysitron is one of the companies that design and sell commercial products for force measurement. TI 900 TriboIndenter is a model they have that looks very similar to our actuation force measurement machine. TI 900 is able to measure

the hardness and elastic modulus of thin films and coating. This machine also can measure force and displacement in two parallel axes to the vibration platform. There are 3 axis motion systems in this machine, however only one axis is enough for the actuation measurement. Travel Range for TI 900 is 150 mm on X direction and 250 mm on Y direction.

5.2.1 Force Measurement Mechanism

Hysitron machine is ability to measure lateral force is up to 2 mN with sensitivity of 3.5 μN and for longitudinal force would be 30 mN with 30 μN . On the other hand in our customized machine the force can measure the lateral force 100 μN . Due to measuring of lateral force in our application it shows that customized machine is more proper in this set of experiments.

5.2.2 Noise and Smooth Motion

Hysitron's stages move with a stepper motor that is specifically designed for them. [14] The mechanism of stepper motors is based on a rotary motion that goes step by step. There are multiple electromagnetic teeth around the main core. The core has a gear shape with teeth around it. In the first step in a two phase mechanism, one of the electromagnets activates, which causes the nearest core tooth to align itself with that electromagnetic tooth. [20] On servo Motors (DC Motor) there are no steps and with it the rotary motion is consistent. That means the stator magnets are permanent magnets and they provide a

consistent magnetic field around the central core. The Rotor (core) generates an alternative magnetic field by external current. This current makes the rotor have a changing magnetic pole and this causes it to attract and repel stators alternatively. [21] The mechanism on these is important because of the type of motion that they provide to the stage. Due to the many steps that a step motor needs to have to make a complete rotation circle, the noise and vibration are much higher when compared with DC motors which have a continuous process. [20], [22] Also, stepper motors are not able to stop immediately.[22]

Moreover, the maximum velocity and acceleration of DC motors are more than stepper motors. Stepper motors are also cheaper and have longer lifetimes when compared with DC motors. Considering the high precision in this measurement process, a stage with a DC motor was considered for the machine in order to have more accurate data.

5.2.3 Accessibility

The Hysitron machine only has a small window on the front side, which makes the working on the test setup hard for the operator. However, in our design there are two wide windows on the front and the side which gives an easy accessibility to most of important components inside the box.

5.2.4 Transparent Box

The advantages of having a transparent box is that enough light can enter into the box and there is no need to install more light. Also, the process is observable and the operator can notice any emergency or system failure by watching it. Hysitron used a blank plastic box that makes the interior box dark.

5.2.5 Clean Room

Keeping the substrate and other components in a clean environment is an essential concern in order to have accurate data. The sealed box used in Hysitron's machine and the enclosure box in our machine protects the test components. However, only our device has positive air flow keeping the dirt and other types of prolusions out while the operator is working inside the box with open windows.

5.2.6 Flexibility

Most of the components in our machine are able to move and be positioned on specific locations. For instance, the structure and the stage are installed on a breadboard that has thread all over its surface, and by undoing their screws the components can be relocated anywhere. The Camera, the sensor, the vacuum grabber and the lateral structure can be adjusted and move. However, Hysitron's machine is based on granite and this prevents it from having the same option. Our sensor is the only component that can move vertically up and down.

5.2.7 Price and Transportation

Hysitron's machine costs almost \$285000, which is a considerable amount of money and shipping such a big and heavy machine also presents a large problem and a large cost. Our machine costs much less than Hysitron's commercial product (around \$15000) and overall is lighter and is easier to transport, as the parts can be undone and assembled easily again.

CHAPTER 6: CONCLUSION

6.1 Conclusion

After doing research about the problems with traditional electrowetting force measurements, the idea of direct measurement encouraged us to start research in this field. As a result we designed a precision machine to be able to measure actuation displacement force as well as electrowetting actuation force. The machine includes a vibration isolation system to reduce disorder effects, an actuation force that is provided by the motion mechanism, a force measurement system with MEMS based sensor technology, adjustment and an enclosure box to increase the accuracy of the experiment. This system is competitive with similar commercial products due to aspects such as lower price, easy setting of motion parameters and recording data by compatibility with LABVIEW software, high repeatability, high accuracy, low scale of noises and simple design.

6.2 Future Work

This machine can be developed under some aspects. One would be to optimize the machine's components to increase the accuracy and measurement capacity.

Moreover the overall size of machine could be smaller and applying the actuation force could be done by different methods such as continues electrowetting or ultra-sonic waves. Increasing the sensitivity and contribution between components is the main key that needs to be followed in future work.

REFERENCES

- [1] Elaine G. Shafrin and William A. Zisman, "constitutive relations in the wetting of low energy surfaces and the theory of the retraction method of preparing monolayers," no. u. s. naval research laboratory, 1959.
- [2] J. R. Rowlinson and B. Widom, molecular theory of capillarity. dover publications, 2003, p. 352.
- [3] T. Chow, "wetting of rough surfaces," journal of physics: condensed matter, vol. 445, 1999.
- [4] B. D. N. Eustathopoulos, M.G. Nicholas, wettability at high temperatures, vol. 1999. elsevier, 1999, p. 420.
- [5] J. Berthier, P. Dubois, P. Clementz, P. Claustre, C. Peponnet, and Y. Fouillet, "actuation potentials and capillary forces in electrowetting based microsystems," sensors and actuators a: physical, vol. 134, no. 2, pp. 471–479, mar. 2007.
- [6] Katherine Marie Smyth, "wetting hysteresis and droplet roll off behavior on superhydrophobic surfaces," massachusetts institute of technology, 2010.
- [7] F. Mugele and J.-C. Baret, "electrowetting: from basics to applications," journal of physics: condensed matter, vol. 17, no. 28, pp. r705–r774, jul. 2005.
- [8] Krüss Co, "measurement contact angle." [online]. available: <http://www.kruss.de/en/theory/measurements/contact-angle/measurement-contact-angle.html>. [accessed: 20-oct-2012].
- [9] P. D. Roger P. Woodward, "contact angle measurements using the drop shape method."
- [10] D. Öner and T. J. Mccarthy, "ultrahydrophobic surfaces. effects of topography length scales on wettability," langmuir, vol. 16, no. 20, pp. 7777–7782, oct. 2000.

- [11] C. W. Nelson, C. M. Lynch, and N. B. Crane, "continuous electrowetting via electrochemical diodes," *lab on a chip*, vol. 11, no. 13, pp. 2149–52, jul. 2011.
- [12] Edmund Optics Co, "compact vis-nir fixed focal length lenses." [online]. available: <http://www.edmundoptics.com/imaging/imaging-lenses/edmund-optics-designed-lenses/compact-vis-nir-fixed-focal-length-lenses/3338>. [accessed: 29-oct-2012].
- [13] Newport Co, "mid-range travel linear stage, steel, 100 mm travel, dc motor, uts series."
- [14] Jean-Baptiste Waldner, *nanocomputers and swarm intelligence*. wiley-ieee press, 2008.
- [15] "how sensors work - mems sensor." [online]. available: <http://www.sensorland.com/howpage023.html>. [accessed: 20-sep-2012].
- [16] Newport Co, "legs and isolators : anatomy of a pneumatic vibration isolation system."
- [17] "thorlabs - performanceplus series, 110 mm (4.3") thick, enhanced stiffness, enhanced damping breadboards." [online]. available: http://www.thorlabs.com/newgrouppage9.cfm?objectgroup_id=1860. [accessed: 22-oct-2012].
- [18] J.-U. Shim, G. Cristobal, D. R. Link, T. Thorsen, Y. Jia, K. Piattelli, and S. Fraden, "control and measurement of the phase behavior of aqueous solutions using microfluidics," *journal of the american chemical society*, vol. 129, no. 28, pp. 8825–35, jul. 2007.
- [19] N. B Crane, Qi Ni, Timo Marschke, Samuel Steele, Seyed Najafi, "contact angle friction and contact angle hysteresis (CAH) through force measurements," in *imece2012*, 2012, pp. 1–3.
- [20] "servo motor guide." [online]. available: <http://www.anaheimautomation.com/manuals/forms/servo-motor-guide.php>. [accessed: 11-oct-2012].
- [21] "clemson vehicular electronics laboratory: dc motors." [online]. available: <http://www.cvel.clemson.edu/auto/actuators/motors-dc.html>. [accessed: 11-oct-2012].

[22] "hybrid motors - vibration and resonance - nmb technologies corporation."
[online]. available: <http://www.nmbtc.com/step-motors/engineering/vibration-and-resonance.html>. [accessed: 11-oct-2012].

APPENDICES

Appendix A: Components Specifications

This appendix shows the full details of the components that were used in the design of this machine. These components are the stage, the camera, the lens, the MEMS sensor, the breadboard, the micro positioners and the controller. Specifications help the designer to choose the best device or component based on the functionality, accuracy, repeatability.

Table A: Stage Specifications (Taken from Newport Co)

Spec	Value	Spec	Value
Model	UTS100CC	Resolution	0.1 μm
Travel Range	100 mm	Pitch	100 or $\pm 55 \mu\text{rad}$
Normal Load Capacity	200 N	Weight	3.2 kg
Minimum Incremental Motion, Linear	0.3 μm	Axial Load Capacity	50 N
On-Axis Accuracy	5.5 or $\pm 2.75 \mu\text{m}$	Thread Type	M4 and M6
Maximum Speed	40 m/s	Motor Type	DC
Bi-direction Repeatability	4 or $\pm 2.0 \mu\text{m}$	Bearings	Linear ball bearings

Appendix A (Continued)

Table B: Camera Specifications (Taken from Edmundsoptic Co)

Specs	Value/Model
Model Number	EO-0413M
Type of Sensor	MT9V032
Camera Sensor Format	1/3"
Sensing Area H x V (mm)	4.5 x 2.8
Pixels H x V	752 x 480
Pixel Size, H x V (µm)	6 x 6
Pixel Depth	8-bit
Frame Rate (FSP)	87
Type of shutter	Global
Synchronization	Internal or Via Software
Video Output	USB 2
Dimensions	44 x 44 x 25.4
Mount	C-Mount
Mounting Thread	1/4- 20

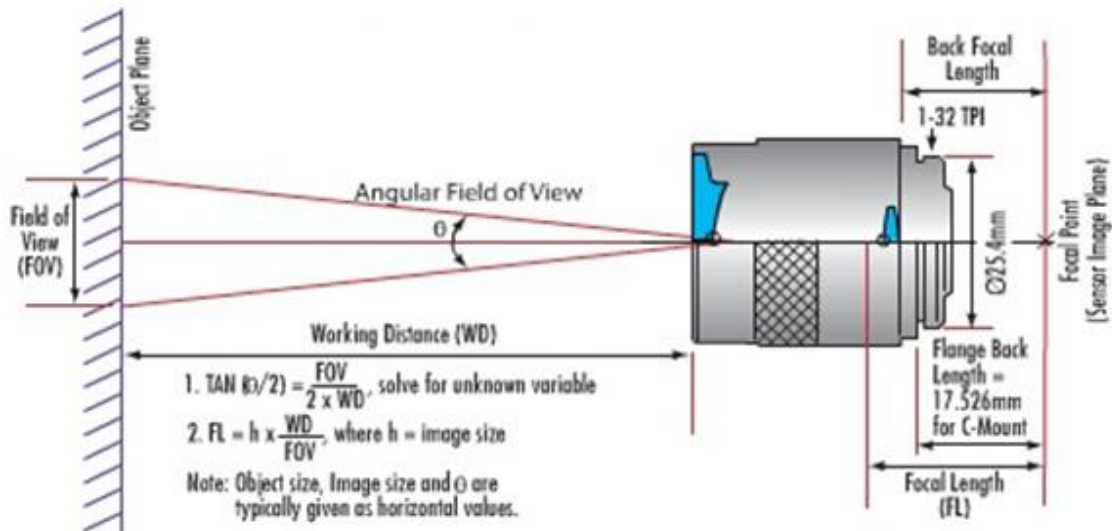


Figure A: Focal Lens Length (Sketch is Taken from Edmundsoptic Co with Permission)

Appendix A (Continued)

Table C: Rail Structure Specifications (Taken from Newport Co)

Specs	Value/Model
Model	X95-0.5
Rail Length	19.69 in. (500 mm)
Width	3.74 in. (95 mm)
Height	3.74 in. (95 mm)
Material	Aluminum
Thread Type	M6
Weight	3.7 lb/ft (5.5 kg/m)

Table D: Rail Carriers Specifications (Taken from Newport Co)

Specs	Value/Model
Model	CXL95-80
Width	6.5 in. (31.5 mm)
Height	1.24 in. (31.5 mm)
Length	3.15 in. (80 mm)
Material	Aluminum
Thread Type	3.15 in. (80 mm)

Appendix A (Continued)

Table E: MEMS Sensor Specifications (Taken from Nanoscience Instrumental Co)

Specs	Value/Model
Model	FTS-100
Force Range	$\pm 100 \mu\text{N}$, 10 mg
Sensitivity / Sensor Gain	50 $\mu\text{N/V}$, 5 mg/V
Output Signal	0 - 5 V
Output Voltage at Zero Load	2.25 V
Power Supply Voltage	5 V
Resolution at 1,000 Hz	0.05 μN , 0.005 mg
Resolution at 10 Hz	0.005 μN , 0.0005 mg
Probe Material	Single Crystal Silicon
Probe Thickness	50 μm
Probe Width	300 μm
Probe Length	3,000 μm
Overall Assembly Dimensions	28 x 8x 5.2 mm

Table F: Breadboard Specifications (Taken from Newport Co)

Specs	Value/Model
Model	RG-34-2
Thread Type	1/4-20
Width	3 ft.
Length	4 ft.
Thickness	2.4 ft.
Mounting Hole pattern	1 in. grid
Surface Flatness	± 0.004 in.
Working Surface	400 Series ferromagnetic stainless steel
Type of shutter	Global
Maximum Dynamic Deflection Coefficient	$< 9.4 \times 10^{-4}$

Appendix A (Continued)

Table G: Manual Positioner Specifications (Taken from Newport Co)

Specs	Value/Model
Model	460A-XZ
Travel Range	0.5 in. (12.7 mm)
Axes of Travel	X, Z
Load Capacity	15 lb. (67 N)
Bearings	Ball Bearings
Material	Aluminum
Thread Type	1/4-20
Load Capacity, Vertical	5 lb. (22 N)
Angular Deviation	<150 μ rad

Appendix B: Customized Components Drawing

There are many customized components that are designed and fabricated in the machine. Mostly these parts are used to mount different components and devices on them.

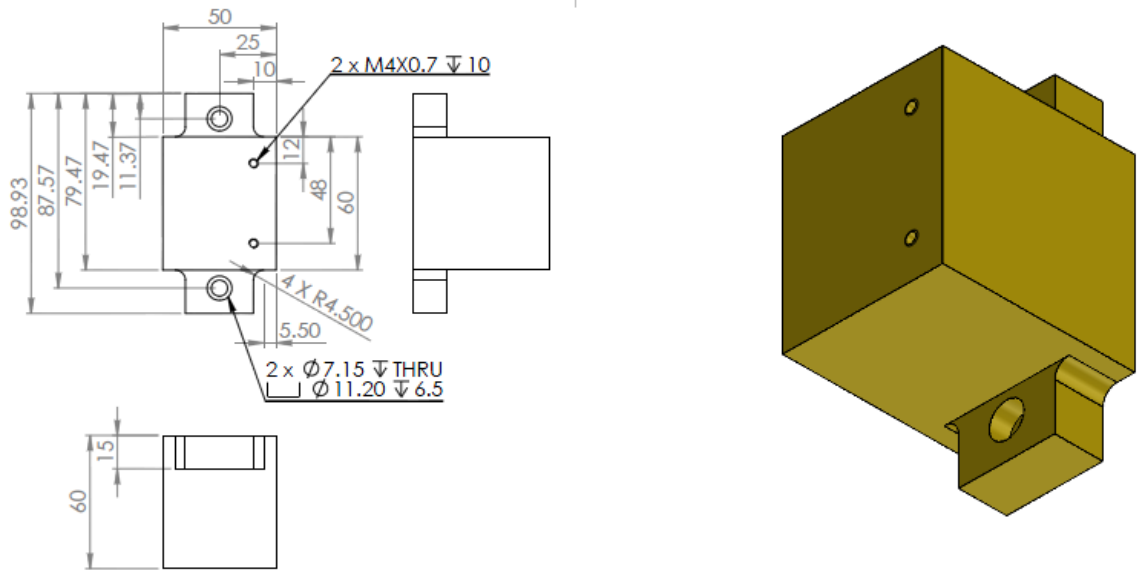


Figure B: Sensor Mount Block

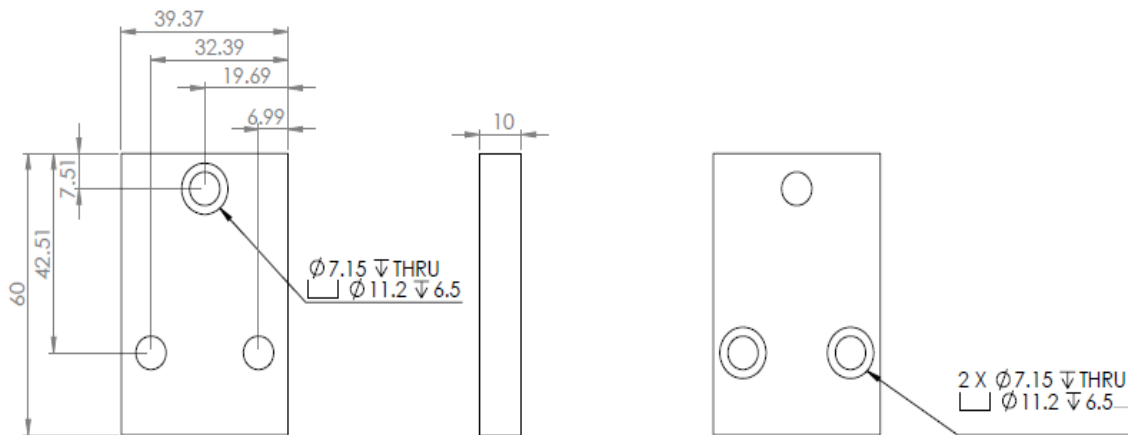


Figure C: Camera Mounting Bracket to Micro Positioner

Appendix B (Continued)

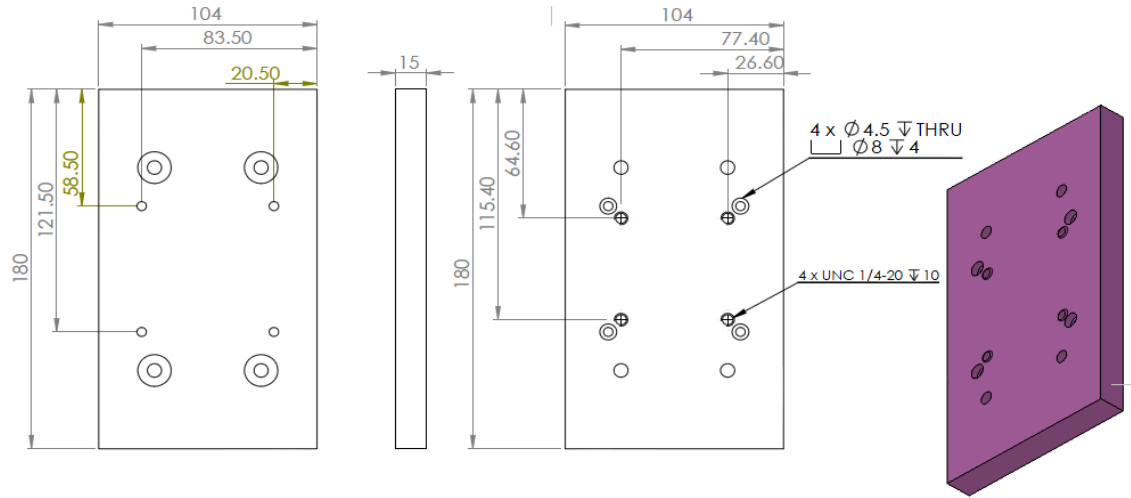


Figure D: Under Stage Bracket

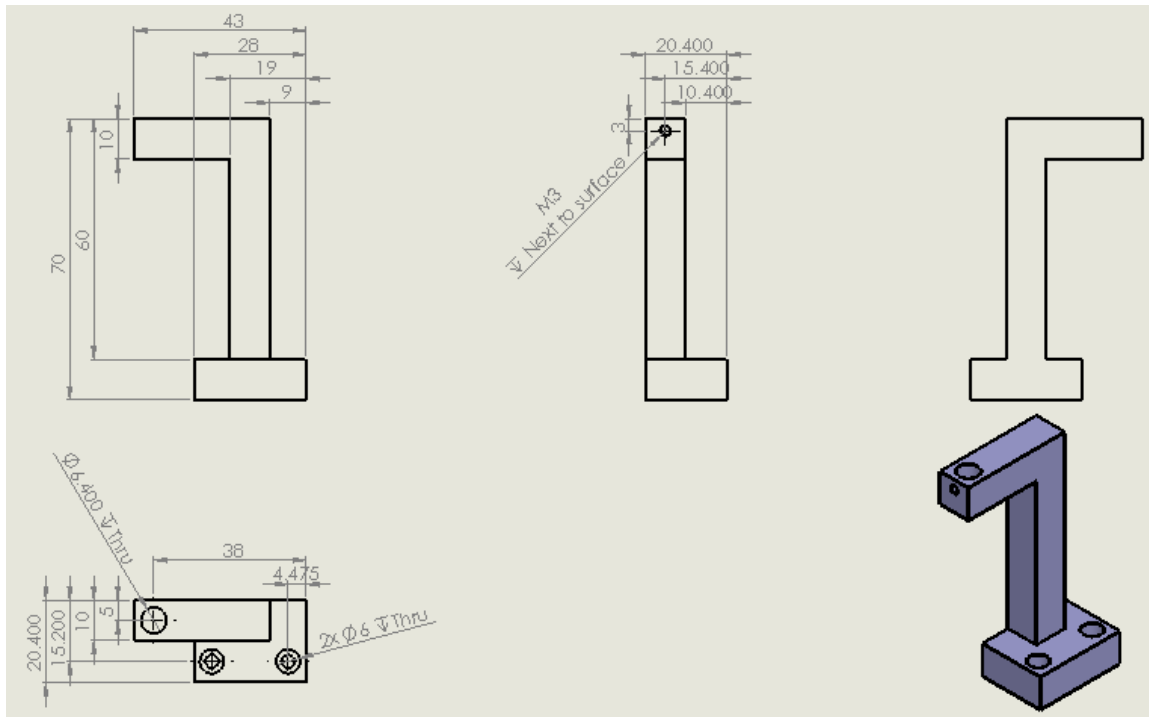


Figure E: Vacuum Lifter Mount

Appendix B (Continued)

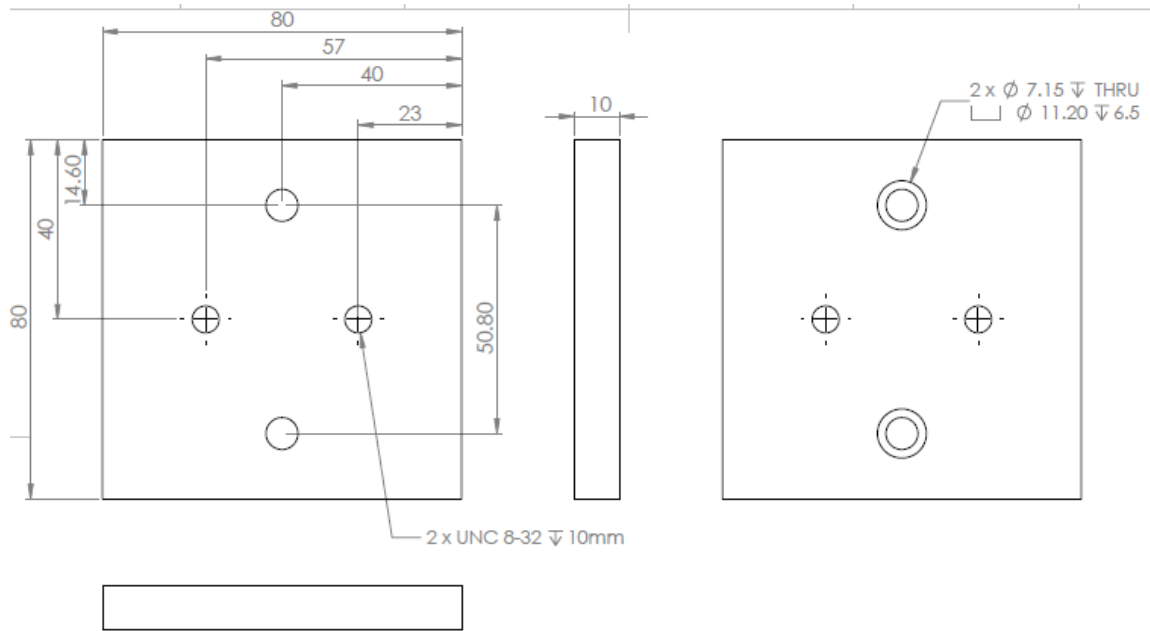


Figure F: Micro Positioner Mounting Bracket to Carrier

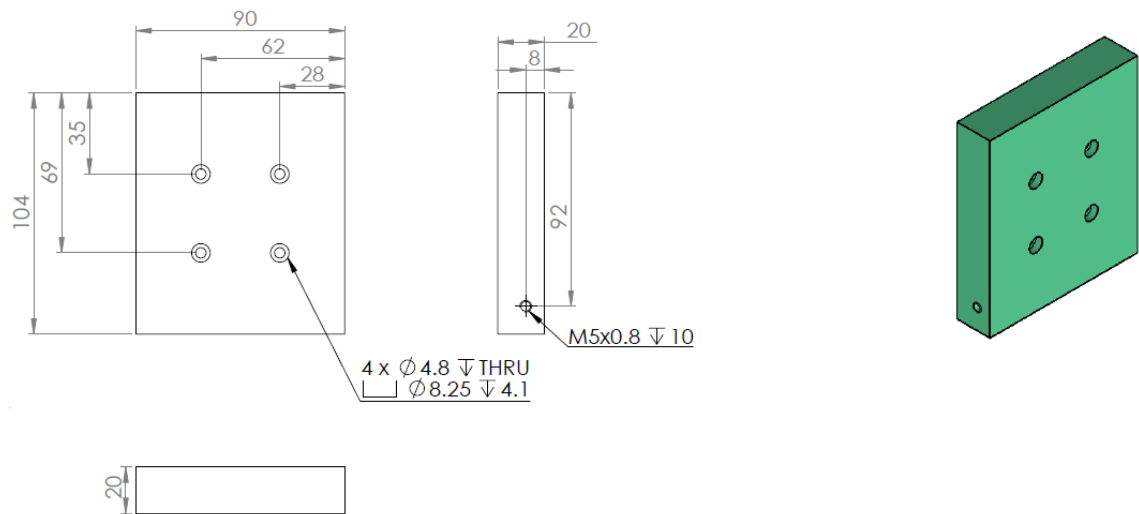








Figure G: Top Stage Bracket

Appendix C: Copyright and Permissions

RE: permission for thesis [T20121004001KS040Z485794] Inbox x  

 **Tan, Sylvia** Sylvia.Tan@newport.com 1:51 PM (7 hours ago) ☆  

to me, Warren, Rochelle, ITSC 

Hi Kamran,

Yes it's fine to use the picture in your thesis.

Best Regards,

Sylvia




Sylvia Tan
Product Specialist, Vibration Control
Office: [949\) 253-1775](tel:9492531775)
Newport Corporation
Experience | Solutions

Newport Corporation Family of Brands – Corion® · New Focus™ · Ophir® · Oriel® Instruments · Richardson Gratings™ · Spectra-Physics®

This message and any attachments thereto are intended only for the designated recipient(s) and may contain confidential or proprietary information and be subject to the attorney-client privilege or other confidentiality protections. If you are not a designated recipient, you may not review, use, copy or distribute this message or any attachments. If you receive this in error, please notify the sender by reply e-mail and permanently delete the original and any copies of this message and any attachments thereto. Thank you.

People (4)

Tan, Sylvia
sylvia.tan@newport.com

[Show details](#)

Figure H: Permission for Figure 12 Courtesy of Newport Co

Appendix C (Continued)

Image credit to Nanoscience Instruments Inbox x

Joe Grech jgrech@nanoscience.com Oct 3 (1 day ago) ☆

to me ▾


Thank you for requesting permission to use images from our website (www.nanoscience.com) for your thesis.

Please feel free to use the images as long as you give proper credit to Nanoscience Instruments.

Thanks,
Joe

.....

Joseph S. Grech
Sales & Marketing Director
Nanoscience Instruments, Inc.
9831 S. 51st Street, Suite C119
Phoenix, AZ 85044 USA
[888-777-5573](tel:888-777-5573) / [480-940-3940](tel:480-940-3940) ext.224
Fax: [480-940-3941](tel:480-940-3941)
jgrech@nanoscience.com
www.nanoscience.com



.....

What's New





Joe Grech
jgrech@nanoscience.com


+ ✉ ▾


[Show details](#)




Figure I: Permission for Figure 11 Courtesy of Nanoscience Instruments Co

Appendix C (Continued)

Re: Edmund Optics images  Inbox    People (2)

 **Gretchen Morris** Greetings, I understand you are interested in using Edmund Optics' graphics i... Oct 15 (3 days ago) ☆

 **Camron Najafi** Hi, I desined a mashine for our academic research and we used a camera and le... Oct 16 (2 days ago) ☆

 **Gretchen Morris** Oct 17 (1 day ago) ☆  

to me ▾

Hello Camron,
I have attached an eps file and a pdf of the artwork I think you have referenced. If this is not what you are looking for, can you provide a direct link to our website or a screen grab of the correct graphic?

When using Edmund Optics' material, it must be accompanied by the following copy:

Image courtesy of Edmund Optics

Best of luck with your project!

Gretchen Morris
Director, Global Catalog Production
Edmund Optics America

Figure J: Permission for Figure A Courtesy of Edmund Optics Co

Appendix C (Continued)

Dallakyan, Taguhi Taguhi.Dallakyan@newport.com
to me

11/30/11

What's New

Hello Camron,

Thank you for your call. Please see below the speed stability data for ILS-LM stages at 0.1mm/sec and 500mm/sec speeds :

Dallakyan, Taguhi

Add to circles

Show details

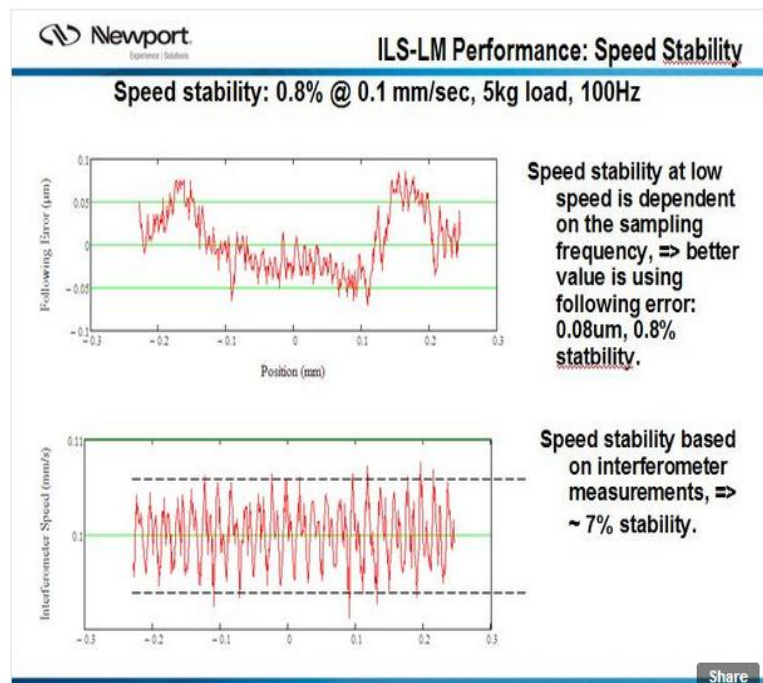


Figure K: Direct Email for Figure 26 Courtesy of Newport Co